

1 **Palaeoecology of Middle Triassic tetrapod ichnoassociations (middle Muschelkalk,**
2 **NE Iberian Peninsula) and their implications for palaeobiogeography in the**
3 **western Tethys region**

4
5 Chabier De Jaime-Soguero^{a,1}, Eudald Mujal^{b,a,1,*}, Jaume Dinarès-Turell^c, Oriol Oms^d,
6 Arnau Bolet^{a,e}, Guillem Orlandi-Oliveras^a, Josep Fortuny^{a,*}

7
8 (a) *Institut Català de Paleontologia Miquel Crusafont, Universitat Autònoma de*
9 *Barcelona, ICTA-ICP building, c/de les columnes s/n, Campus de la UAB, E-08193*
10 *Cerdanyola del Vallès, Catalonia, Spain*

11 (b) *Staatliches Museum für Naturkunde Stuttgart, Rosenstein 1, D-70191 Stuttgart,*
12 *Germany*

13 (c) *Istituto Nazionale di Geofisica e Vulcanologia, Via di Vigna Murata 605, I-00143*
14 *Roma, Italy*

15 (d) *Departament de Geologia, Universitat Autònoma de Barcelona, E-08193 Bellaterra,*
16 *Catalonia, Spain*

17 (e) *School of Earth Sciences, University of Bristol, Wills Memorial Building, Queens*
18 *Road, Bristol BS8 1RJ, United Kingdom.*

19
20 (1) These authors contributed equally to this work

21 *Corresponding authors: eudald.mujalgrane@smns-bw.de (E. Mujal),
22 josep.fortuny@icp.cat (J. Fortuny)

23
24 **Abstract**

25 Tetrapod ichnology is a powerful tool to reconstruct the faunal composition of Middle
26 Triassic ecosystems. However, reconstructions based on a single palaeoenvironment
27 provide an incomplete and impoverished picture of the actual palaeodiversity. In this
28 paper, we analyse Middle Triassic tetrapod ichnoassociations from the detrital
29 Muschelkalk facies of the Catalan Basin of northeast Spain, ranging from terrestrial to
30 coastal settings. We identified two main tetrapod ichnoassociations, preserved in two
31 different palaeoenvironments, comprising the following ichnogenera and morphotypes:
32 *Procolophonichnium*, *Chelonipus*, *Rhynchosauroides*, *Rotodactylus*, *Chirotherium*,
33 *Isochirotherium*, *Sphingopus*, and indeterminate chirotheriids. We also statistically
34 analyse a database of all known Middle Triassic tetrapod footprint localities worldwide;

35 this database includes, for each track locality, the precise age, the palaeoenvironment
36 and the presence/absence of ichnotaxa. Our results on the composition of ichnofauna
37 within the palaeoenvironments of the Catalan Basin are integrated into this database.
38 This approach allows us to revisit the palaeoenvironmental bias linked to the marine
39 transgression that affected the Western Tethys region. Tetrapod ichnoassociations reveal
40 the following palaeoenvironmental patterns: (1) in coastal settings, ichnoassociations
41 are *Rhynchosauroides*-dominated and diversity is relatively low; (2) in terrestrial
42 settings and those with less marine influences, ichnoassociations are non-
43 *Rhynchosauroides*-dominated, usually characterised by more abundant chirotheriid
44 tracks and, generally, a higher track diversity. The correlation between tetrapod
45 ichnoassociations and sedimentary facies reveals how palaeoenvironmental constraints
46 influenced faunal assemblages, especially those of the Middle Triassic of the Western
47 Tethys region. Ichnoassociations allow the ecological response of tetrapod faunas to the
48 environmental changes to be inferred for this critical time interval. Marine
49 transgressions strongly influenced tetrapod ecosystems: environmental conditions were
50 key for the faunal recovery in the aftermath of the end-Permian extinction, with the
51 settlement of the so-called modern faunas and the rise of the dinosaur lineage.

52

53 **Keywords**

54 tetrapod footprints; palaeoenvironments; coastal settings; Anisian; Ladinian; equatorial
55 Pangaea

56

57 **1. Introduction**

58 The Triassic period is characterised by recovery in the aftermath of the most
59 severe biotic crisis of Earth history, the end-Permian mass extinction, which led to the
60 origin of so-called modern ecosystems (Benton, 2016). However, the complete faunal
61 recovery was delayed until the Middle Triassic due to the harsh environmental
62 conditions (Irmis and Whiteside, 2012), especially in equatorial Pangaea (Sun et al.,
63 2012; Benton and Newell, 2014; Benton, 2018). While in the marine realm the severity
64 of the biotic crisis and subsequent recovery are relatively well understood, the
65 magnitude of the event is still uncertain for the continental ecosystems, especially
66 considering vertebrates (Lucas, 2017, 2018). The Middle Triassic continental vertebrate
67 faunas globally present a relatively high diversity, with the radiation of newly
68 successful diapsid groups (Ezcurra, 2010), the lineages of which most probably

69 appeared during the late Palaeozoic (Simões et al., 2018; Bernardi et al., 2019). On the
70 one hand, the Lower–Middle Triassic tetrapod record from middle-high palaeolatitudes
71 is particularly well-known, based on the great sampling efforts performed in South
72 Africa and Russia, which reveal that these ecosystems were characterised by abundant
73 temnospondyl amphibians, as well as therapsids, being neodiapsid reptiles present, but
74 less abundant (Lucas, 2010; Romano et al., 2020, and references therein). On the other
75 hand, Middle Triassic continental vertebrate faunas from equatorial Pangaea include
76 temnospondyl amphibians (e.g., capitosaurids and plagiosaurids) and a high diversity of
77 reptiles ranging from terrestrial to semi-aquatic and aquatic habitats (Sues and Fraser,
78 2010). Dominant diapsid reptiles (particularly archosauromorphs) coexisted with
79 procolophonid parareptiles, stem-turtles, lepidosauromorphs and a few cynodonts
80 (Schoch and Milner, 2000; Damiani et al., 2009; Ezcurra, 2010; Schoch and Sues, 2015,
81 2018; Schoch et al., 2018; Simões et al., 2018). Environmental changes through time,
82 including a greater marine influence, are reflected by coastal and marine vertebrate
83 faunas, such as tanystropheids (e.g., *Macrocnemus* and *Tanystropheus*), stem turtles,
84 ichthyosauriforms, thalattosaurians, sauropterygians (e.g., pachypleurosaurs,
85 nothosaurians and placodonts), saurosphargids, as well as fish faunas (actinopterygians
86 and sarcopterygians) (Rieppel and Hagdorn, 1998; Rieppel, 2000; Ezcurra, 2010; Xing
87 et al., 2020). Terrestrial ecosystems and the role of their faunas are far from being fully
88 understood because of the small number of sites, although some exceptional *Fossil-*
89 *Lagerstätten* localities exist (Schoch and Seegis, 2016). In fact, the number of terrestrial
90 taxa from Middle Triassic low-latitude localities is generally sparse (Lucas, 2010;
91 Fortuny et al., 2011a).

92 The skeletal information of Middle Triassic terrestrial faunas is complemented
93 by a notably richer tetrapod ichnological record. Continental Middle Triassic vertebrate
94 footprints are globally recorded (Fig. 1) in many palaeoenvironments ranging from
95 inland fluvial and lacustrine settings to coastal (shores, lagoons, tidal flats) and shallow
96 marine settings (Table S1). Therefore, ichnofaunal diversity may broadly reflect the
97 habitat preferences of vertebrates, as well as environmental changes through space and
98 time, as it is observed in other time intervals (Mujal et al., 2016a, 2017a, 2017b;
99 Bernardi et al., 2018; Marchetti et al., 2019a). In fact, tetrapod footprints are useful tools
100 in palaeoenvironmental analyses (Melchor and Sarjeant, 2004; Hunt and Lucas, 2007a,
101 2007b; Diedrich, 2008; Melchor, 2015; Marchetti et al., 2017, 2019b; Mujal et al.,
102 2018a; Schneider et al., 2020). Noteworthy, biases in the ichnofaunal record also exist,

103 as is the case for the Triassic amphibian temnospondyl record, with abundant bones and
104 scarce footprints (Klein and Lucas, 2010a; Marsicano et al., 2014; Mujal and Schoch,
105 2020; Farman and Bell, 2020; Schneider et al., 2020).

106 Important changes took place during the Middle Triassic in the western peri-
107 Tethys region: most of the earliest Triassic terrestrial ecosystems of the central-eastern
108 part of Pangaea (nowadays Europe and northern Africa) evolved to coastal-marine
109 environments (Bourquin et al., 2011). This was due to the marine transgression that
110 affected most of the European and North-African basins (Escudero-Mozo et al., 2015;
111 Franz et al., 2015) (Fig. 1). This transgression was not coeval in all these basins as
112 revealed by the diachronic nature of the facies (López-Gómez et al., 2002; Franz et al.,
113 2013, 2015; Ortí et al., 2017, 2018; Maron et al., 2019), resulting in diachronous faunal
114 changes. The record of Middle Triassic vertebrate footprints from the Western peri-
115 Tethys basins is significantly abundant (Fig. 1; Table S1), with localities known from
116 Spain (Demathieu et al., 1978; Pérez-López, 1993; Gand et al., 2010; Fortuny et al.,
117 2011a; Díaz-Martínez et al., 2015; Mujal et al., 2015, 2018a; Reolid and Reolid, 2017;
118 Berrocal-Casero et al., 2018a, 2018b; Reolid et al., 2020), Morocco (Klein et al., 2011),
119 Algeria (Kotański et al., 2004), Tunisia (Niedźwiedzki et al., 2017), France (Demathieu
120 and Demathieu, 2004; Gand et al., 2007, and references therein), Italy (Avanzini and
121 Mietto, 2008; Avanzini et al., 2011; Citton et al. 2020; Mietto et al., 2020, and
122 references therein), Switzerland (Klein et al., 2016; Cavin and Piuz, 2020, and
123 references therein), the Netherlands (Demathieu and Oosterink, 1983, 1988; Diedrich,
124 2002, 2008; Marchetti et al., 2019c) and Germany (e.g., Haubold, 1971a, 1971b, 1984;
125 Haubold and Klein, 2002; Diedrich, 2008, 2012; Klein et al., 2015; Klein and Lucas,
126 2018; Marchetti et al., 2020; Mujal and Schoch, 2020).

127 In order to understand the relationship of Middle Triassic vertebrate faunas, in
128 particular those from the Western Tethys, with the palaeoenvironment, we provide a
129 detailed analysis of the ichnological record from the middle Muschelkalk unit of the
130 Catalan Basin (NE Iberian Peninsula). Such unit corresponds to a coastal and distal
131 alluvial succession embedded within the two (lower and upper) Muschelkalk marine
132 carbonate units (Calvet and Marzo, 1994; see section 2 below). So far, Muschelkalk
133 terrestrial ichnoassemblages from the Iberian Peninsula are scanty (Fortuny et al.,
134 2011a), only known from two middle Muschelkalk sites from the Catalan Basin (Mujal
135 et al., 2015, 2018a), and two additional Muschelkalk sites from the Iberian Ranges
136 (Demathieu et al., 1987; Berrocal-Casero et al., 2018a, 2018b). This work significantly

137 enlarges the knowledge of the Middle Triassic vertebrate ichnofaunas from the Iberian
138 Peninsula by describing three new ichnosites.

139 As a whole, we pursue to understand tetrapod palaeoecology on the basis of the
140 ichnological record, i.e., how palaeoenvironments constrain the distribution of
141 ichnotaxa, either prompting an abundant presence or the complete absence of specific
142 ichnotaxa (e.g., Diedrich, 2008; Melchor, 2015; Mujal et al., 2018a). Additionally,
143 because sea level fluctuations caused strong changes on these ecosystems, the present
144 work sheds light on the vertebrate footprint palaeoecology according to: (1) the newly
145 discovered tetrapod ichnoassemblages, in relation to their stratigraphic and
146 sedimentological setting, from the Catalan Basin (Texts S1 and S2); (2) the Western
147 Tethys tetrapod ichnological record. The integrated review of Middle Triassic tetrapod
148 tracks and corresponding palaeoenvironments sheds light on the evolution of a key time
149 interval for the tetrapod evolution in an area, the equatorial Pangaea, in which the
150 skeletal record is scanty.

151

152 **2. Geological setting**

153

154 During the Middle Triassic, the Iberian plate was situated in the western peri-
155 Tethys, eastern part of Pangaea, equatorial latitudes (Fig. 1). The Catalan Coastal
156 Ranges (CCR, NE Iberian Peninsula; Fig. 2) were a depressed, tectonically controlled
157 zone (a rift system) known as the Catalan Basin, corresponding to the north-eastern
158 region of the Iberian plate (Marzo, 1980). The CCR evolved as a NE-SW oriented rift
159 with conjugate NW-SE fault systems (Galán-Abellán et al., 2013). During this time
160 interval, all western peri-Tethys basins were intersected by marine transgressions
161 (occurring at different times as indicated by the diachronic facies at European scale) that
162 resulted in the formation of shallow epicontinental sea areas (Escudero-Mozo et al.,
163 2015; Ortí et al., 2017).

164 As regards the Iberian plate, the Early to early Middle Triassic terrestrial
165 ecosystems are represented by the siliciclastic Buntsandstein red-beds facies mostly
166 corresponding to alluvial and fluvial deposits (e.g., Dinarès-Turell et al., 2005;
167 Bourquin et al., 2011; Fortuny et al., 2011b; Galán-Abellán et al., 2013; Mujal et al.,
168 2016b, 2017a, 2017b). These facies were gradually replaced by shallow marine
169 environments from East to West, represented by the carbonate and evaporitic
170 Muschelkalk facies (Escudero-Mozo et al., 2015). During the Anisian–Ladinian

171 transition, a short regression episode took place in eastern Iberian plate, leading the
172 marine areas of the Catalan Basin to evolve to coastal environments, such as tidal mud
173 flats, sabkhas and distal floodplains (Calvet and Marzo, 1994; Ortí et al., 2017, 2018).
174 Later, a new transgression took place, affecting most parts of Iberia during the Ladinian
175 (Escudero-Mozo et al., 2015) (Fig. 1). In the sedimentary record, the
176 palaeoenvironments of the regression interval are represented by detrital deposits
177 composed of mudstone and sandstone red-beds with gypsum and limestone/dolostone
178 intervals between the two carbonate units of the Muschelkalk facies (Calvet and Marzo,
179 1994; Morad et al., 1995; Mujal et al., 2015, 2018a; Ortí et al., 2018). Thus, in the
180 Catalan Basin, three Muschelkalk (informal) units are well-differentiated: lower, middle
181 and upper Muschelkalk facies.

182 The thickness of the Triassic (Buntsandstein, Muschelkalk and Keuper)
183 successions of the Catalan Basin ranges from 500 to 800 m (Calvet et al., 1990). The
184 Middle Triassic Muschelkalk successions are arranged in three different domains, from
185 SW to NE: Priorat-Baix Ebre, Prades and Gaià-Monsteny (Marzo, 1980). The newly
186 herein reported tetrapod footprint localities, as well as those studied by Mujal et al.
187 (2015, 2018a) are all found in the Gaià-Montseny domain. The middle Muschelkalk
188 facies successions, which in several areas are highly affected by alpine tectonics
189 deformations, present an average thickness of about 100 m (Calvet and Marzo, 1994)
190 (Fig. 2). These facies are dated as late Anisian–middle Ladinian based on palynomorph
191 and conodont biostratigraphy (Solé de Porta et al., 1987; Márquez-Aliaga et al., 2000).
192 The middle Muschelkalk facies consist of a mixed succession of siliciclastic, carbonate
193 and evaporitic lithologies. According to Ortí et al. (2018), the succession can be divided
194 in three main basin-scale units: Lower (Paüls Gypsum), Middle (Arbolí Gypsum/Guanta
195 Sandstone) and Upper (Camposines Gypsum). For the detailed descriptions of each unit,
196 especially regarding the evaporitic content, see Morad et al. (1995) and Ortí et al.
197 (2018). The stratigraphic and sedimentological framework for the published (Mujal et
198 al., 2015, 2018a) and new track-bearing successions are described and discussed in
199 sections 4.1 and 5.1 below and Texts S1 and S3. All the tetrapod footprint localities
200 correspond to the Middle Unit of the middle Muschelkalk, specifically to the Arbolí
201 Gypsum and/or the Guanta Sandstone, within the Gaià-Montseny domain. In this
202 domain, according to Ortí et al. (2018):

203 1) The Arbolí Gypsum, mainly corresponding to the lowermost part of the Middle
204 Unit, is a succession of massive, laminated and/or nodular gypsum alternated with

205 red mudstones and discrete greyish dolostone intervals. It is interpreted as “an
206 extensive, evaporitic, red mudflat lodging a mosaic of shallow salinas and sabkhas
207 fed by marine water. This evaporitic mudflat was sensitive to record depositional
208 cyclicity of high-frequency” (Ortí et al., 2018:167).

209 2) The Guanta Sandstone, encompassing most of the Middle Unit, consists of a mainly
210 cyclic red-bed siliciclastic succession of fine- to medium-grained sandstones
211 alternated with mudstones. The sedimentary setting is interpreted as “midfan
212 distributive channels and floodplains of ephemeral streams in sandy alluvial fans”
213 (Ortí et al., 2018:172). As described and discussed (see sections 4.1 and 5.1 below
214 and Texts S1 and S3), these deposits were also influenced by salty waters.

215

216 **3. Material and methods**

217

218 A total of five middle Muschelkalk tetrapod footprint localities from the Catalan
219 Coastal Ranges (NE Iberian Peninsula) are here analysed, together with reference
220 sections by Ortí et al. (2018) (Fig. 2). The track-bearing localities are named, from
221 south to north and west to east (according to their position within the Catalan Basin), as
222 follows: *Penya Rubí* – new locality (Vallirana, Baix Llobregat), *Puigventós* – new
223 locality (Vacarisses, Vallès Occidental), *Collcardús* (Vacarisses, Vallès Occidental;
224 from Mujal et al., 2015), *Pedrera de Can Sallent* (Castellar del Vallès, Vallès
225 Occidental; from Mujal et al., 2018a), *Montmany* – historical finding and new locality
226 (*Figaró-Montmany*, Vallès Oriental).

227 While carrying out the palaeontological prospections, stratigraphic sections have
228 been measured by means of a Jacobs staff and a measuring tape (when possible, as some
229 outcrops are highly tectonised, see below). Some X-ray diffractions were carried out to
230 check dolomite content in dolostones from *Penya Rubí*. The stratigraphic position and
231 the GPS coordinates of the footprint-bearing localities have also been recorded. The
232 exact geographic and stratigraphic origin of the historical finding from the *Montmany* is
233 unknown. However, this area has been recently prospected, and several layers bearing
234 tetrapod footprints, as well as *ex situ* track-bearing slabs, have been discovered. The
235 historic specimen of *Montmany*, a previously unpublished sandstone slab bearing
236 several tetrapod ichnites in convex hyporelief, was located in the fossil collections of
237 the University of Montpellier (France) in 2014 by one of the authors (EM). It has a label
238 from the Museu Geològic del Seminari of Barcelona (MGSB) with catalogue number

239 26310; the label indicates that it was donated in 1975 to the Montpellier institution. In
240 this regard, under the corresponding permits, it was returned to the MGSB in 2018.

241 The new trace fossils recovered from *Penya Rubí*, *Puigventós* and *Montmany*
242 were consolidated for proper conservation with ethyl silicate when necessary, and are
243 stored at the Institut Català de Paleontologia Miquel Crusafont (ICP, Sabadell,
244 Catalonia, Spain). Descriptions and measurements follow the conventions of Haubold
245 (1971a, 1971b) and Leonardi (1987). The specimens used for the ichnotaxonomic
246 assignments are those with a higher degree of morphological preservation (see
247 Marchetti et al., 2019b). Skin impressions preserved in some of the herein analysed
248 footprints are also described in detail and compared to those reported in the literature.
249 Selected ichnites were digitised to obtain 3D models using photogrammetry technique.
250 Photographs were obtained using a digital reflex camera Nikon D3200, with an
251 objective AF-S Nikkor 15-55 mm 1:3.5-5.6 GII and following the procedures of
252 Falkingham (2012) and Mallison and Wings (2014). 3D models were processed with
253 different softwares, following the procedures of Mujal et al. (2016a, 2020): Agisoft
254 Photoscan (standard v.1.1.4) to generate the dense point cloud and the mesh, MeshLab
255 (v.2016.12 and v.2020.07) to edit the mesh (cleaning, scale and orientation) and
256 ParaView (v.4.1.0) to generate colour depth maps and contours.

257 A database of the worldwide known Middle Triassic tetrapod tracksites has also
258 been built (Table S1), including for each region/locality: age, inferred
259 palaeoenvironment and ichnotaxa present. Descriptive statistics have been performed
260 based on relative abundance (Tables S2, S3), counting presence (1) and absence (0) of
261 each ichnotaxon in the different palaeoenvironments. We calculated the percentages of
262 occurrence of each ichnotaxon, without considering the absolute number of footprints
263 from the analysed regions/localities. In this sense, the representativity of each
264 ichnotaxon in a certain setting is calculated by dividing its occurrences within that
265 palaeoenvironment by all the occurrences reported from this type of palaeoenvironment
266 (Table S2). Also, the percentage of occurrence of a specific ichnotaxon in a determinate
267 palaeoenvironment is calculated as its occurrences in a certain palaeoenvironment by
268 the number of localities assigned to this palaeoenvironment (Table S3).

269 Tetrapod ichnogenera are taken as the basic counting unit, because they are the
270 best defined ichnotaxonomic level, though some exceptions are also considered. Less
271 precisely identified trace fossils are also counted, because some tetrapod trace
272 morphotypes may bear relevant information regarding the distribution of the potential

273 tracemakers. They include: Dinosauromorpha tracks and tridactyl tracks (the latter may
274 correspond to poorly preserved chirotheriids or dinosauromorphs as well); and
275 indeterminate chirotheriid tracks, because in some localities these are not identified at
276 ichnogenetic level, but such ichnorecord indicates the presence of relatively large
277 archosaurs. Similarly, tetrapod swimming traces, even if they encompass different
278 producers (and include different ichnogenera; e.g., Xing et al., 2020), are also counted
279 as their presence is indicative of a peculiar locomotion gait, and thus provide
280 information on the palaeoenvironmental setting, and on the taphonomy of track bearing
281 localities.

282 Palaeoenvironmental settings of each locality/region are classified into four
283 major groups, from proximal to distal: 1) alluvial/inland (including fluvial and
284 lacustrine deposits), 2) distal alluvial/supratidal (including playa lake and coarse-
285 grained sabkha deposits), 3) coastal/tidal flats (including fine-grained sabkha or sabkha-
286 like deposits), and 4) shallow marine. The criteria to classify these settings follow the
287 palaeoenvironmental analyses of each work (see references in Table S1), including
288 specific palaeoenvironmental definitions and, especially in the absence of precise
289 information, the sedimentary characteristics of the facies preserving tetrapod traces. In
290 addition, in the case of palaeoenvironments defined as continental-marine transition
291 without further specification, we consider those composed of fine- to very fine-grained
292 and carbonate facies in the coastal group, whereas those composed of coarser facies are
293 put in the distal alluvial group. Regarding sabkha or sabkha-like settings, we follow a
294 similar rule: those with finer facies are in the coastal group, and those with coarser
295 facies are in the distal alluvial group. This responds to the fact that the coarser deposits
296 are considered as more proximal than the finer deposits. Notwithstanding, we might
297 expect further palaeoenvironmental interpretations of the track-bearing localities in
298 future works in order to refine these analyses.

299

300 *3.1. Institutional abbreviations*

301

302 IPS, Institut Català de Paleontologia Miquel Crusafont (formerly, Institut de
303 Paleontologia de Sabadell), Sabadell, Catalonia, Spain.

304 MGSB, Museu Geològic del Seminari de Barcelona, Barcelona, Catalonia,
305 Spain.

306

307 **4. Results**

308

309 *4.1. Stratigraphy and sedimentology*

310

311 The newly discovered tetrapod footprint localities of *Penya Rubí*, *Puigventós*
312 and *Montmany*, all from the middle *Muschelkalk* facies, are briefly described here. For
313 extended description and interpretation of each outcrop, see Text S1. Furthermore, our
314 results on the stratigraphy and sedimentology of those facies are compared with those
315 from *Ortí et al. (2018)* and references therein, along with those derived from the
316 tracksites described in *Mujal et al. (2015, 2018a)*. Figure 2 summarizes the stratigraphic
317 position of the tracksites within the middle *Muschelkalk* succession.

318 The *Penya Rubí* outcrop (Fig. 3) includes a stratigraphic succession up to ~27 m
319 thick and encompasses the Lower Unit (*Paüls Gypsum*) and part of the Middle Unit
320 (*Arbolí Gypsum* and *Guanta Sandstone*). The succession presents a terrestrialization
321 trend (Fig. 3A). The lowermost part consists of whitish gypsum deposits overlying the
322 lower *Muschelkalk* carbonates. They correspond to the *Paüls Gypsum*. The overlying
323 deposits consist of alternating and finely laminated reddish mudstones and very fine- to
324 fine-grained sandstones. In between this reddish succession there is a distinct interval
325 (~50 cm thick) of finely laminated greyish mudstones and dolostones (Fig. 3A, B),
326 which laterally become coarser and display cross lamination (Fig. 3C). The red layers
327 commonly display cross lamination (including unidirectional, wave and climbing
328 ripples) (Fig. 3D). Some intervals preserve abundant load and water escape structures
329 (Fig. 3E). All in all, these red deposits mostly show bidirectional water currents and
330 periods of rapid sedimentation. The surfaces of the greyish interval occasionally display
331 wrinkle structures (elephant skin-like textures; Fig. 3F), may indicating periods of low
332 energy environmental conditions. This part of the succession was mostly deposited
333 under subaqueous conditions and/or the substrate was mostly water saturated (high
334 moisture), though sporadic dryer episodes or seasons might also took place. We
335 interpret these deposits as most probably representing intertidal and *sabkha*-like areas,
336 where finely laminated microbial mats (Fig. 3B, G) were developed (greyish deposits
337 and dolostones), and correspond to the *Arbolí Gypsum*. Most of the tetrapod footprints
338 from *Penya Rubí* (i.e., those of relatively small size) are preserved on the surfaces of the
339 grey carbonate (dolostone) microbial mat deposits (lower arrow in Fig. 3A, and Fig. 3G,
340 H); yet the first reddish sandstones and mudstones also preserve sparse small-sized

341 tetrapod footprints, as well as a xiphosuran traceway (De Jaime-Soguero et al., 2020).
342 Notably, the large archosaur footprints are preserved at the basal surface of the mud-
343 cracked, medium-grained sandstone (upper arrow in Fig. 3A), representing the onset of
344 the Guanta Sandstone (see Text S1 and S3). Our interpretations match those by Calvet
345 and Marzo (1994), Mujal et al. (2018a) and Ortí et al. (2018), suggesting that during the
346 marine regression the Catalan Basin was a vast tidal flat, with a low relief that included
347 a mosaic of environments ranging from subtidal to supratidal areas (Ortí et al., 2017)
348 (see Text S1 for further details). The topmost part of the succession is built up of tabular
349 reddish medium-grained sandstones with cross stratification and red laminated
350 mudstones and fine-grained sandstones (Fig. 3A). This succession denotes a marked
351 palaeoenvironmental change towards a more terrestrial setting that represents the onset
352 of the Guanta Sandstone. Noteworthy, the succession of Pedrera de Can Sallent (see
353 Mujal et al., 2018a) can be generally compared to that of Penya Rubí, especially in
354 terms of granulometry, sedimentary structures, and strata arrangement: strata are finely
355 laminated, wave (bidirectional) ripples are common, and wrinkle structures most
356 probably induced by microbial activity are also present. Otherwise, the Pedrera de Can
357 Sallent succession differs with that of Penya Rubí in the main lithological composition:
358 the former is more siliciclastic than the latter. This difference may be explained by the
359 palaeogeographic position of the localities within the Catalan Basin (see Ortí et al.,
360 2018; Texts S1 and S3).

361 The tectonization of the Puigventós outcrop (Fig. 4A) prevents the measuring of
362 a complete stratigraphic succession with confidence (though a composite section is
363 fairly possible; Fig. 2). The main lithological and sedimentological features reveal
364 closer similarities to the medium-grained sandstone at the top of the succession of
365 Penya Rubí (Guanta Sandstone; upper half in Fig. 3A) rather than to the underlying
366 fine-grained intervals (Arbolí Gypsum; lower half in Fig. 3A). The Puigventós
367 succession mostly consists of reddish fine- to medium-grained sandstones usually with
368 cross stratification and lamination that are interbedded with red mudstones. Wave
369 ripples are common, and occasional mud-cracked surfaces and moulds of hopper
370 crystals also occur. Bioturbation produced by invertebrates (consisting in both vertical
371 and horizontal burrows) is especially abundant in some sandstone layers. In general
372 terms, the succession is similar to that of Collcardús, previously reported by Mujal et al.
373 (2015), and located just 5 km eastwards. The Collcardús outcrops are composed of red
374 bed deposits corresponding to mudstones alternated with fine- to medium-grained

375 sandstones, often with cross stratification, ripples and, occasionally, desiccation cracks
376 (Mujal et al., 2015). Based on these features (see Text S1 for further details), we
377 interpret the palaeoenvironmental setting of Puigventós (and Collcardús) as a distal
378 alluvial area with frequent desiccation periods and with highly salty waters, but also
379 with flooding (at least periodical) events, which is consistent with the presence of
380 tetrapod swimming traces. The studied outcrop might correspond to the Guanta
381 Sandstone, although a short interval in the lowermost part could correspond to the
382 Arbolí Gypsum. In general terms, the Puigventós succession is here interpreted as a
383 proximal sabkha plain or a tidal mixed-flat (with notable terrestrial or terrigenous
384 influence, as denoted by a major presence of siliciclastic deposits), except for the
385 basalmost part, which it was probably more similar to the tidal flats of Peña Rubí.

386 The succession of Montmany (Fig. 4B–J) is similar to that of Puigventós and
387 Collcardús as well. The main components of the succession are decimetre-thick reddish
388 fine- to medium-grained sandstones, with cross stratification and lamination,
389 interbedded with red mudstones deposits ~0.5 to 1 m thick (Fig. 4B). Within sandstone
390 layers, wave ripples are common structures, but climbing and unidirectional flow
391 ripples are also present (Fig. 4C). Most of the tetrapod footprints are found on the basal
392 surfaces of the sandstone layers (Fig. 4D), tetrapod swimming traces (though not very
393 abundant) are also preserved. As in Puigventós, some sandstone layers are highly
394 bioturbated (Fig. 4E), with both vertical and horizontal sinuous burrows commonly with
395 meniscate infill. Other more occasional structures are wrinkled surfaces probably of
396 microbial mats (Fig. 4E), mud-cracks (Fig. 4G), moulds of large gypsum nodules (Fig.
397 4H) and of hopper crystals, all these being indicative of desiccation periods. Otherwise,
398 water escape and load structures (Fig. 4I) are also present, suggesting rapid flooding and
399 increase of the sedimentation rate and higher energy of the system. Of note, potential
400 xiphosuran traces have been identified in Montmany (IPS120436 and IPS120437),
401 further pointing to connections to the palaeocoast, though Triassic xiphosurid
402 ichnofossils are known from far inland settings in the nearby Pyrenean Basin (Mujal et
403 al., 2018b). These traces will be studied in future works and compared with the
404 xiphosuran traceway already described at the Peña Rubí locality (De Jaime-Soguero et
405 al., 2020). A distinct 25 cm thick massive carbonate layer (probably a dolostone) bears
406 *Rhynchosauroides tirolicus* Abel, 1926 footprints in concave epirelief, being different to
407 the rest of the succession (left *in situ*; arrow in Fig. 4J). According to all the mentioned
408 features, this succession may be equivalent to those of Puigventós and Collcardús,

409 mostly corresponding to the Guanta Sandstone. In this case, the facies correspond to a
410 distal alluvial setting, being a proximal sabkha plain, with salty waters and with
411 frequent desiccation periods, but also periods of flooding and a relatively strong
412 terrigenous input. Nonetheless, as indicated by Ortí et al. (2018), some intervals (such
413 as the carbonate layer) may correspond to interdigitated parts of the Arbolí Gypsum
414 (Fig. 2C).

415

416 4.2. *The middle Muschelkalk track record of the Catalan Basin*

417

418 Numerous tetrapod tracks have been recovered from the Peña Rubí, Puigventós
419 and Montmany outcrops. They are assigned to at least 10 different ichnotaxa.
420 Specimens of the same ichnotaxon but from different localities may display distinct
421 features, though in some cases differences appear to be related to substrate composition,
422 as discussed below and in Text S3. In this section we briefly describe each tetrapod
423 ichnotaxon of the middle Muschelkalk ichnoassemblage from the Catalan Basin, mainly
424 from the three newly reported localities (Peña Rubí, Puigventós and Montmany), but
425 also including remarks from the previously described localities of Collcardús (Mujal et
426 al., 2015) and Pedrera de Can Sallent (Mujal et al., 2018a). The detailed systematics of
427 each ichnotaxon, as well as additional figures are provided in the supplementary
428 information (Text S2, Figs. S1–S10).

429 Tracks of *Procolophonichnium haarmuehlensis* (Holst et al., 1970) have been
430 identified in the Peña Rubí locality by relatively small, pentadactyl and
431 semiplantigrade impressions (Figs. 5A, S1). The digit proportions and relative position
432 make their imprints wider than long. The digit imprints shape is moderately robust and
433 straight to distally curved outwards. The length of digit impressions increases from I to
434 III, with digit IV imprint slightly shorter than digit III. The imprint of digit I is the
435 shortest. The imprint of digit V is separated from the others and more proximally
436 positioned, and its length is subequal to digit II (Klein et al., 2015). Claw impressions
437 are preserved in all digits, being deeply impressed and markedly curved outwards.
438 Awaiting further analyses, including the study of relative depth patterns (e.g., Mujal et
439 al., 2020), procolophonid parareptiles and therapsid synapsids are considered the most
440 probable producers of *P. haarmuehlensis* (Klein et al., 2015; Marchetti et al., 2019c).

441 Three small-sized ichnites from Montmany have been referred to
442 *Procolophonichnium* sp. (Figs. 5B, S2). They are pentadactyl and plantigrade, with

443 robust and straight to slightly bent outwards digits imprints displaying relatively large
444 clawed tips. The lateral portion of the footprints is relatively deeply impressed,
445 suggesting a different trackmaker to those of *P. haarmuehlensis*.

446 Several footprints assigned to an indeterminate ichnospecies of *Chelonipus*
447 Rühle von Lilienstern, 1939 have been recovered from Puigventós and Montmany
448 localities (Figs. 5C, S2A, D, S3). As observed in the studied specimens, this ichnogenus
449 is characterised by a relatively wide trackway, with a low pace angulation (Haubold,
450 1971a; Lovelace and Lovelace, 2012; see Lichtig et al., 2018 for a review of the
451 ichnogenus). The footprints outlines are represented by roundish proximally concave
452 arches, with imprints of the digit tips usually displaying a dragging trail traces anteriorly
453 directed. The imprints are digitigrade to semiplantigrade and wider than long. The digit
454 impressions are short and with round tips. Pes tracks display three to five digits
455 impressions, while manus tracks show up to four digit impressions. A characteristic
456 feature is the impression of the interdigital area between digits II, III and IV. The
457 potential trackmaker of *Chelonipus* is traditionally referred to turtles (Lichtig et al.,
458 2018). Nevertheless, other potential producers, such as temnospondyl amphibians (e.g.,
459 Mujal and Schoch, 2020) or other unknown producers cannot be discarded.

460 The most abundant morphotype of the middle Muschelkalk is *Rhynchosauroides*
461 Maidwell, 1911 (Figs. 3G, H, 5D, E, F, S4, S5). This ichnotaxon is featured by
462 relatively small, lacertoid-like and markedly ectaxonic tracks, with slender digit
463 impressions. In both manus and pes tracks, the imprints of digits I to IV increase in
464 length and are curved inwards, while digit V imprint (similar to digit I in length) is
465 separated, more proximally positioned and rotated outwards. The manus impressions
466 tend to be semiplantigrade (occasionally digitigrade to semidigitigrade), with digit
467 imprints relatively shorter and wider than those of pes impressions. Pes tracks are
468 mainly digitigrade to semidigitigrade; most commonly only composed by the
469 impression of digits II, III and IV. Pes tracks anterolaterally or laterally overstep manus
470 tracks. All the footprints from Peña Rubí and Pedrera de Can Sallent (Mujal et al.,
471 2018), most of those from Puigventós, and those from the carbonate layer of Montmany
472 (see Text S2 for details on the specimen numbers) fall into the range morphology of *R.*
473 *tirolicus*, which is well known from Middle Triassic coastal fine-grained and carbonate
474 deposits of the Italian Southern Alps (e.g., Avanzini and Renesto, 2002; Valdiserri and
475 Avanzini, 2007; Mietto et al., 2020), and possibly from Germany (e.g., Diedrich, 2002,
476 2008). Otherwise, the relatively poor preservation of other specimens from Montmany

477 and Puigventós (e.g., Figs. 5F, S5), as well as Colcardús (Mujal et al., 2015), precludes
478 an ichnospecific identification. The large chronological and palaeobiogeographical
479 occurrence of *Rhynchosauroides* may suggest that different taxa could have produced
480 these characteristic lacertoid-like tracks, most likely being small neodiapsids, including
481 lepidosauromorphs and/or archosauromorphs (e.g., Avanzini and Renesto, 2002;
482 Diedrich, 2002, 2008; Valentini et al., 2007; Mujal et al., 2018).

483 Tracks of *Rotodactylus* Peabody, 1948 have been recovered from Peña Rubí
484 and Puigventós localities (Figs. 5G, 6C, S6, S8). These footprints are digitigrade, longer
485 than wide, pentadactyl and relatively small. The digit length increases from I to IV.
486 Imprints of digits I to IV are straight, subparallel, with the tips markedly bent inwards.
487 Imprint of digit V is only represented with a round impression in a far proximal position
488 from the rest of the imprint, being a characteristic feature of this ichnogenus (Peabody,
489 1948; Haubold, 1971a; Klein and Lucas, 2010a; Niedźwiedzki et al., 2013).
490 Dinosauromorphs are considered the potential trackmakers of *Rotodactylus* (e.g.,
491 Peabody, 1948; Haubold, 1967, 1999; Haubold and Klein, 2002; Brusatte et al., 2011;
492 Niedźwiedzki et al., 2013); non-dinosauromorph archosauromorphs have also been
493 proposed as producers (Padian, 2013), although a thorough track-trackmaker correlation
494 for this alternative attribution is not available so far.

495 The largest tetrapod ichnites recovered from the middle Muschelkalk of the
496 Catalan Basin belong to the ichnofamily Chirotheriidae. Two ichnospecies of
497 *Chirotherium* Kaup, 1835 have been recovered. Both morphotypes are characterised by
498 pes tracks with tightly grouped imprints of digits II, III, IV, being digit III the longest,
499 and with digit I imprint slightly separated and more proximally. Imprints of digits I to
500 IV are straight and distally tapering, with relatively large triangular claw impressions.
501 Digit V imprint is separated from the others, more proximally positioned and rotated
502 outwards. These are diagnostic features of *Chirotherium*, a very common morphotype
503 from Lower and Middle Triassic terrestrial deposits and with a global distribution
504 (Haubold, 1971a, 1984; Klein and Haubold, 2007; Klein and Lucas, 2010b; Díaz-
505 Martínez and Pérez-García, 2012; Lagnaoui et al., 2019; Xing and Klein, 2019).

506 From Montmany, two manus-pes sets of relatively small tracks with slender
507 (elongated) shape are conferred to *Chirotherium sickleri* Kaup, 1835 (Figs. 6A, S2A,
508 D). Pes tracks are semiplantigrade and manus tracks are semidigitigrade. In pes tracks,
509 digit II imprint is notably shorter than digit IV imprint. Manus tracks are smaller than
510 pes tracks, but with similar digit proportions and more anteriorly positioned. Pes tracks

511 are slightly outward rotated in comparison with the manus impressions, a feature
512 characteristic of this ichnospecies, and opposite to *C. barthii* (e.g., Klein and Lucas,
513 2010a; Klein et al., 2016). “Rauisuchian” (pseudosuchian) archosauriforms are possible
514 trackmakers of this ichnospecies (Klein and Lucas, 2010a).

515 The second ichnospecies recovered is *Chirotherium barthii* Kaup, 1835, found
516 in Puigventós and in the medium-grained sandstone stratum of Penya Rubí (upper arrow
517 in Fig. 3A, Figs. 6B, S7). Pes tracks are semiplantigrade and relatively large. The
518 diagnostic features of this ichnospecies (e.g., Haubold, 1971b, 2006; Klein and Lucas,
519 2010a) observed in the Catalan specimens are: the longest digit III impression, followed
520 by digit II and a clearly shorter digit IV imprint; the triangular, large claw impressions
521 of the pedal digits; the pedal digit V imprint outlining a large, deeply impressed oval-
522 shaped proximal pad, and thinning distally. Pseudosuchian archosaurs or stem
523 archosaurs are the potential trackmakers of this ichnospecies (Haubold, 2006; Haubold
524 and Klein, 2000, 2002; Klein and Haubold, 2003; Klein et al., 2011).

525 A single left pes track from Puigventós is referred to *Isochirotherium* Haubold,
526 1971a (Figs. 6C, S8). It is semiplantigrade and pentadactyl imprints, with robust digits
527 with rounded claw impressions. Imprints of digits I to IV are straight and subparallel,
528 wider on the middle-distal portion, being somewhat oval-shaped. The digit III imprint is
529 the longest, with the digit II imprint subequal in length. Imprint of digit IV is much
530 shorter, but longer than the impression of digit I imprint. These four digit imprints form
531 a compact group. The impression of digit V is separated from the others, proximally
532 positioned slightly curved outwards and a laterally orientated. Among *Isochirotherium*
533 ichnospecies, *I. coureli* (Demathieu, 1970) is the most similar to that from Puigventós
534 (e.g., Gand et al., 2007; Klein and Lucas, 2018). Despite the fact that the absence of the
535 typical large pad in the imprint of digit V (due to breakage of the slab) and the lack of
536 manus impressions make the ichnospecies identification uncertain, the *Isochirotherium*
537 tracks of Puigventós display the same features as that of Collcardús (see Mujal et al.,
538 2015). In addition, one of the tracks recovered in Collcardús preserves a large pad
539 impression of the digit V, also characteristic of *I. coureli*. Thus, we assign all
540 *Isochirotherium* tracks of the middle Muschelkalk from the Catalan Basin to *I. cf.*
541 *coureli*. The potential trackmakers of *Isochirotherium* were archosaurs, as in
542 *Chirotherium*, though no skeletal counterparts are so far correlated to this ichnogenus
543 (Klein and Lucas, 2010a).

544 Several tracks recovered from Montmany and a single partial track from
545 Puigventós are attributed to *Sphingopus ferox* Demathieu, 1966 (Figs. 4C, D, 6D, S9).
546 The pes tracks are semiplantigrade with a characteristic functionally tridactyl trend, with
547 the predominating imprints of II, III and IV. The manus of this ichnogenus is located in
548 an inner position regarding the pes tracks. The diagnostic features of this ichnospecies
549 (e.g., Demathieu, 1966, 1985; Haubold and Klein, 2002; Gand et al., 2007; Klein and
550 Lucas, 2018) observed in the Catalan specimens are: the longest digit III imprint,
551 followed by a notably shorter digit II imprint, which is longer than digit IV imprint; the
552 relatively low angle of digits II and IV (27°–38°, mean of 31°); the impression of digit I
553 more proximally positioned respect to digits II–IV, located behind digit II imprint and
554 rotated outwards; the digit V imprint, being curved and rotated outwards, and more
555 proximally positioned than and clearly separated from the other digit imprints; the
556 smaller manus tracks positioned at the height of pedal digit III imprint and on the inner
557 side of pes tracks. This ichnotaxon has been related to dinosauiromorph trackmakers
558 (Haubold and Klein, 2000; Haubold and Klein, 2002; Brusatte et al., 2011).

559 Moreover, several tracks from Puigventós and Montmany localities display
560 features characteristic of chirotheriid ichnotaxa (e.g., Demathieu and Demathieu, 2004;
561 Haubold and Klein, 2002) (Fig. S10). However, due to their poor and incomplete
562 preservation, and/or because they are isolated manus tracks (Fig. S10A), these ichnites
563 cannot be assigned to any ichnogenus. Of interest, some of these tracks were probably
564 impressed under swimming locomotion (Figs. S2D, S10B), a behaviour already known
565 from the Triassic archosaur ichnological record (e.g., Thomson and Droser, 2015; Mujal
566 et al., 2017a).

567

568 4.3. Distribution of the Middle Triassic track record: descriptive statistics

569

570 Table S1 consists in a database of the global Middle Triassic tetrapod track
571 occurrences, including up to 75 regions/areas/localities. On its basis, a counting study of
572 the presence/absence of the tetrapod ichnorecord in each region reveals a total of 329
573 tetrapod trace occurrences classified in 29 different morphotypes (mostly ichnogenera
574 but also other specific cases, see methods in section 3 above). Following the
575 palaeoenvironmental classification used in this work, 33% of the localities correspond
576 to inland settings, 32% to distal alluvial, 28% to coastal, and 7% to shallow marine (Fig.
577 S11). Noteworthy, a very few track occurrences are classified in the shallow marine

578 setting; therefore, the obtained results may suffer changes with future field data from
579 such settings. Despite the similar proportions of the three most represented
580 palaeoenvironments, the inland and distal alluvial settings accumulate, respectively, the
581 36.78% (121) and 34.35% (113) of all ichnological occurrences. The coastal settings
582 record the 25.84% (85) of the total occurrences, and shallow marine environments only
583 account for the 3.04% (10) of the total occurrences (Table S2). Also, the tetrapod
584 ichnodiversity recorded in distal alluvial (26 morphotypes) and inland (23 morphotypes)
585 settings is clearly higher than in those of the coastal (16 morphotypes) and shallow
586 marine (6 morphotypes) settings (Table S2). It should be noted that shallow marine
587 settings mainly yield swimming traces, which are not distinguished at a detailed
588 ichnotaxonomic level, though clearly different ichnogenera and ichnospecies are
589 included within swimming traces (for thorough descriptions of tetrapod swimming
590 ichnotaxa, see Xing et al., 2020, and references therein; see also Table S1).

591 Figure S12 shows that, among all the tetrapod trace occurrences analysed, the
592 dominant ichnogenera are: *Rhynchosauroides* (16.11%), *Chirotherium* (13.68%),
593 *Isochirotherium* (10.33%), *Procolophonichnium* (7.90%), *Rotodactylus* (7.29%), and
594 *Synaptichnium* (6.38%). Also, swimming traces morphotypes (4.56%) and
595 *Chirotheriidae* indet. tracks (4.26%) tend to be frequent in Middle Triassic outcrops.
596 The occurrence of the remaining tetrapod ichnogenera and morphotypes is relatively
597 low (each one representing <4% of the total occurrences) (represented within “Others”
598 in Fig. S12). Of note, the relative proportions of each ichnotaxon in each
599 palaeoenvironment (Fig. 7A) show the palaeoenvironmental distribution of each
600 tetrapod trace morphotype without considering the total number of footprints in each
601 region (i.e., counting only presence/absence of each morphotype in each region).
602 Therefore, these data reflect the tetrapod ichnodiversity, but not the relative abundance
603 of each ichnotaxa/morphotypes.

604 Figure 7B shows the total number of occurrences of each tetrapod
605 ichnotaxon/morphotype (see also Tables S2 and S3), *Rhynchosauroides* occurrences are
606 higher in coastal settings than in distal alluvial and alluvial settings.
607 *Procolophonichnium* shows the same trend with a proportionally higher presence in
608 coastal palaeoenvironments than in the other ones. The occurrences of *Chirotherium*
609 and *Isochirotherium* have a very similar trend to each other, being more abundant in
610 distal alluvial and inland palaeoenvironments, the opposite trend to those of
611 *Rhynchosauroides* and *Procolophonichnium*. The distribution of *Synaptichnium*

612 occurrences should be taken with caution, as some tracks assigned to
613 “*Brachychirotherium*” may correspond to the former ichnogenus (or to *Chirotherium* as
614 well; see discussion in Klein and Lucas, 2010b, 2018). The number of Chirotheriidae
615 indet. track occurrences is markedly higher in inland palaeoenvironments than in the
616 other ones (i.e., following the trend of the identified chirotheriid ichnogenera). Lastly,
617 occurrences referred to swimming traces show a relatively homogeneous distribution
618 through all palaeoenvironments. Table S3 shows the percentage of occurrence of each
619 morphotype in each palaeoenvironmental setting (taking into account the number of
620 localities from this palaeoenvironment). *Rhynchosauroides* and *Procolophonichnium*
621 have a markedly higher occurrence in coastal environments (90.5% and 57.1,
622 respectively) than in distal alluvial (66.7% and 29.2%, respectively) and alluvial (64.0%
623 and 24.0%, respectively) palaeoenvironments. This is, tracks of these two ichnogenera
624 are more frequently found in deposits corresponding to coastal settings than those of
625 distal alluvial and alluvial ones. As with the total number of occurrences, the
626 percentages of chirotheriid track occurrences are inverse to *Rhynchosauroides* and
627 *Procolophonichnium*, being higher in inland and distal alluvial palaeoenvironments than
628 in the coastal ones. *Rotodactylus* occurrences show a slight increase towards inland
629 settings, though it is not as marked as that of chirotheriid ichnotaxa. Therefore, Tables
630 S2 and S3 generally show the same proportions in number of occurrences and
631 percentage of occurrences for each ichnotaxon in each palaeoenvironments.

632 A comparison of the proportions of the different tetrapod morphotypes in each
633 palaeoenvironment (Fig. 7B) shows that *Rhynchosauroides* and *Procolophonichnium*
634 are proportionally more abundant in coastal settings than in distal alluvial and inland
635 palaeoenvironments. Such proportion decrease of these ichnogenera towards inland
636 settings is reverse to the tetrapod ichnodiversity (Table S2), which increases from
637 coastal to distal alluvial and inland settings (Fig. 8). Otherwise, the presence of
638 chirotheriid ichnotaxa (including *Chirotherium*, *Isochirotherium* and Chirotheriidae
639 indet.) and *Rotodactylus* increase in those palaeoenvironmental settings that have a
640 higher diversity.

641 Summarising, we can observe how the palaeoenvironmental distribution and
642 proportions of *Rhynchosauroides* and *Procolophonichnium* is generally inverse to that
643 of chirotheriids and to the track diversity (Figs. 7B, 8). This is especially well-reflected
644 by the tetrapod ichnoassociations of the Middle Triassic Western Tethys, which
645 represent the bulk of data of the analysed localities (Table S1).

646

647 **5. Discussion**

648

649 *5.1. Palaeoecology of the middle Muschelkalk tetrapod ichnoassociations*

650

651 In the Catalan Basin, the onset of the detrital siliciclastic middle Muschelkalk
652 deposits over the marine carbonate succession of the lower Muschelkalk mirrors a
653 regression of the Tethys during the late Anisian–early Ladinian. Areas such as
654 Puigventós and Montmany (Fig. 4) record a succession of changing/alternating
655 environmental settings, ranging from relatively low energy conditions and evaporation
656 periods (i.e., during the development of hopper crystals, gypsum nodules and
657 desiccation cracks) to floodings and events of increased energy with water currents
658 (medium- to coarse-grained thick bedded sandstones with cross stratification; as well as
659 the presence of abundant vertical invertebrate burrows, and horizontal sinuous burrows
660 as well). In the palaeoenvironments of the Puigventós and Montmany successions,
661 relatively large archosaur tracks are found (*Chirotherium*, *Isochirotherium* and
662 *Sphingopus* ichnogenera, as well as indeterminate chirotheriid tracks), even if extensive
663 surfaces are not exposed. This most probably indicates that their trackmakers were
664 common inhabitants of these environments. In contrast, the relatively low presence of
665 *Rhynchosauroides* indicates that their trackmakers (generally small-sized diapsid
666 reptiles) were much less abundant and/or that the preservation of their more gracile
667 footprints was difficult. Even if taphonomic and sampling biases exist, they alone
668 cannot explain the low proportion of *Rhynchosauroides* footprints in these settings
669 (being much less abundant than the chirotheriid tracks; Figs. 7, 8, Text S2), especially if
670 tracks of this ichnogenus dominate in nearby localities (i.e., Peña Rubí and Pedrera de
671 Can Sallent). In this regard, the preservation of skin and claw impressions in the
672 *Chirotherium barthii* specimen IPS85803 indicates that the substrate was able to record
673 small and delicate details and structures, which could include small-sized tetrapod
674 footprints. These observations support the hypothesis that environmental conditions
675 constrained the spatial or areal distribution of tetrapods. Furthermore, *Rotodactylus*
676 tracks (with sizes similar to those of *Rhynchosauroides*) are more abundant in
677 Puigventós than in Peña Rubí, denoting a similar distribution to that of chirotheriid
678 tracks. This is, even if *Rotodactylus* specimens are of small size, they are more abundant
679 in deposits that appear not to favour their preservation. Therefore, the low presence of

680 *Rhynchosauroides* is probably not caused by a low potential of preservation of small-
681 sized footprints, but by an actual low presence of their trackmakers. Moreover, some of
682 the Puigventós slabs containing *Rhynchosauroides* (e.g., IPS110267 and IPS110269)
683 display thin laminae, similar to the microbial mats of Penya Rubí (see below). In the
684 same way, the tracks of *Rhynchosauroides tirolicus* from the Montmany locality are
685 only found in a distinct carbonate layer (interbedded within a red bed succession of
686 mudstones and sandstones; Fig. 4J), where no other ichnotaxa have been observed. This
687 could also denote a palaeoecology-related distribution of this ichnogenus, since it is
688 more common within certain lithologies of various settings that are different from those
689 characterising the Puigventós and Montmany successions. In a qualitative approach,
690 these observations on the presence/absence and relative abundance of ichnotaxa agree
691 with the expected results applying the census methods of Marchetti et al. (2017): poorly
692 exposed surfaces of the Puigventós and Montmany successions (Fig. 4A, B, D), as well
693 as the sandstone layer from the upper portion of the Penya Rubí succession (upper
694 arrow in Fig. 3A), (usually) only preserve relatively large (archosaur) footprints,
695 whereas the carbonate layers of the lower portion of the Penya Rubí succession (lower
696 arrow in Fig. 3A; see below) preserve only small-sized ichnotaxa (dominated by
697 *Rhynchosauroides tirolicus*). These distinct distributions are also found in the
698 previously described middle Muschelkalk localities from the Catalan Basin: the surface
699 of Collcardús (Mujal et al., 2015) contains seven footprints of chirotheriids and one of
700 *Rhynchosauroides*, whereas on the surfaces of Pedrera de Can Sallent (Mujal et al.,
701 2018a) all footprints are of *Rhynchosauroides* (*R. tirolicus*, according to the reanalysis
702 of the present work; see Text S2), except of a single and poorly preserved indeterminate
703 footprint of a relatively large size.

704 In contrast to Puigventós, Montmany and Collcardús, the very fine-grained and
705 carbonate finely-laminated deposits of the Penya Rubí locality presents extremely
706 abundant *Rhynchosauroides tirolicus* footprints (Fig. 3G, H), whereas chirotheriid
707 tracks are absent in the very same layers. *Procolophonichnium* and *Rotodactylus* are
708 present, although these track morphotypes are much less abundant. The presence of
709 microbial mats in the sedimentary succession of Penya Rubí might have prompted the
710 high-quality preservation of the ichnites, including the preservation of scale prints, even
711 if the trackmakers of *Rhynchosauroides* and *Procolophonichnium* were lightweight
712 organisms. In fact, in present day intertidal areas with growing of microbial mats,
713 Carmona et al. (2011) correlated the preservation of tiny details of footprints (in their

714 case, skin of birds' feet) with the presence of thin microbial mats. Such good quality of
715 preservation in microbial mats may depend on the specific environmental conditions,
716 water content and mat overgrowth, affecting the rheological properties of the substrate
717 (Marty et al., 2009; Marchetti et al., 2019b). We therefore suggest that the Peña Rubí
718 fossil footprints underwent similar formation and preservation processes (microbial
719 mats are also finely laminated), within a similar environment, as that reported by
720 Carmona et al. (2011). A similar high-quality preservation of tetrapod tracks is found in
721 the Anisian successions of Winterswijk, the Netherlands (Demathieu and Oosterink,
722 1983, 1988; Marchetti et al., 2019c) and Southern Alps, Italy (Avanzini, 2000; Mietto et
723 al., 2020). Similar experimental analyses on the preservation of footprints on microbial
724 mats carried out by Marty et al. (2009) could also explain the virtually absence of large
725 ichnotaxa: their trackmakers would have moved with difficulties on such substrates,
726 being too inconsistent to support the weight of large organisms.

727 From the *Rhynchosauroides*-dominated tracksite of Pedrera de Can Sallent,
728 Mujal et al. (2018a) documented three different types of footprint preservation
729 correlated to the substrate rheology and environmental variations. In this regard, most
730 samples of the *Rhynchosauroides* from Peña Rubí would be a mix between
731 preservation type 2 (high number of footprints) and preservation type 3 (high level
732 definition in a small sampling) of Mujal et al. (2018a). The high quality of most
733 footprints would be enhanced by the presence of microbial mats (e.g., Marty et al.,
734 2009; Carmona et al., 2011; Marchetti et al., 2019b). The high abundance of footprints,
735 moreover, may have resulted from a combination of: (1) increased activity of the
736 trackmakers (i.e., environment favourable for their presence), implying that the
737 trackmakers would be gregarious as suggested by Demathieu and Demathieu (2004)
738 (see also Diedrich, 2008; Mujal et al., 2016b, 2018a); (2) high preservation potential
739 because of the presence of microbial mats, implying a potential overrepresentation of
740 trackmakers in cohesive substrates exposed during a relatively long period (i.e., time
741 averaging of substrates, see Falkingham, 2014). An additional explanation for the
742 abundance of *Rhynchosauroides* is that this ichnogenus was probably produced by
743 several different small- to medium-sized “lacertoid-like” taxa (neodiapsids, including
744 archosauromorphs and lepidosauromorphs), which would have been common
745 inhabitants of the Middle Triassic coastal settings (cf. Ezcurra, 2016). In this sense, the
746 high presence of *Rhynchosauroides* might be a reflection of an expansion of reptiles that
747 printed similar ichnites and adapted to coastal areas and/or continental floodplains (Fig.

748 8). Even if coastal settings were more favourable to the presence of *Rhynchosauroides*
749 trackmakers, they were also present in alluvial settings (Fig. 7, Table S1; see also
750 discussion above). This indicates that trackmakers were adapted to a wide range of
751 environments and/or that *Rhynchosauroides* encompass a wide range of trackmakers.
752 The latter is also supported by the fact that the time span of this ichnogenus is very
753 long, from the late Permian to the Late Jurassic (Valentini et al., 2007; Avanzini et al.,
754 2010; Lucas, 2019; Marchetti et al., 2019d; Schneider et al., 2020). As noted in section
755 4.2 above and Text S2, the *Rhynchosauroides* tracks on IPS110265 from Puigventós are
756 different from the other specimens from the same locality and from those of the nearby
757 Peña Rubí and Pedrera de Can Sallent localities. This could be related to the presence
758 of a different trackmaker, being the trackmakers of the imprints on IPS110265 from a
759 more inland setting than the others.

760 Other tetrapod ichnotaxa, not as abundant as those previously discussed, also
761 appear to be linked to specific palaeoenvironments (Table S1). *Procolophonichnium*
762 *haarmuehlensis* tracks are only found, together with *Rhynchosauroides*, in the microbial
763 mat layers of Peña Rubí. This ichnospecies is more commonly found in coastal or
764 marine-influenced palaeoenvironments, although it is also present in terrestrial or more
765 inland settings, such as those from Spain, Germany and Morocco (see Klein et al.,
766 2015). In addition, the *Chelonipus* specimens from the Puigventós locality represent the
767 first Middle Triassic record of the ichnogenus outside Germany, where it is present
768 within coastal settings (Lichtig et al., 2018). *Chelonipus* is also known from older
769 terrestrial Triassic localities from the USA (Lovelace and Lovelace, 2012), as well as
770 from coastal ichnosites of the Upper Triassic of Spain (Reolid et al., 2018) and
771 Germany (Lichtig et al., 2018). *Rotodactylus*, although present in both fully terrestrial
772 and coastal-influenced palaeoenvironments, is more abundant in the terrestrial ones (see
773 further discussion in section 5.2 below).

774 An interesting occurrence is that of potential dinosauriforms (*Sphingopus ferox*)
775 in the Montmany and Puigventós successions. These footprints further support former
776 studies and inferences that this group was already present during the Middle Triassic, as
777 also suggest the occurrences of *Sphingopus* from France (see Gand et al., 2007),
778 Germany (Haubold and Klein, 2000, 2002; Klein and Lucas, 2018) and Poland
779 (Brusatte et al. (2011). Further material may help to elucidate the palaeoenvironmental
780 distribution and general evolution of the group, as well as the nature of the potential
781 trackmakers.

782 To sum up, the different middle Muschelkalk localities here surveyed and
783 reviewed suggest that the *Rhynchosauroides*-dominated ichnoassociations were
784 generally linked to low energy environments with more marine influence, such as
785 intertidal flats, as well as distal sabkha plains (see also Mujal et al., 2018a). As already
786 suggested (Diedrich, 2002, 2008; Mujal et al., 2018a), a separate ichnocoenosis for
787 *Rhynchosauroides* may characterise the Middle Triassic coastal settings. On the
788 contrary, the Chirotheriidae-bearing ichnoassociations likely correspond to more
789 terrestrial environments (although still with marine influence), such as alluvial plains
790 and inland sabkha settings (Fig. 13). Of note, the two ichnoassociations of Playa Rubí
791 (lower and upper) mirror the change from the Arbolí Gypsum to the Guanta Sandstone,
792 representing the onset of a more terrestrial environment (see Text S3 for further
793 discussion and details) and thus prompting the appearance of chirotheriid tracks.

794

795 5.2. Middle Triassic tetrapod palaeoecology and palaeobiogeography of the Western 796 Tethys

797

798 The palaeoenvironmental distribution of tetrapod ichnotaxa within the middle
799 Muschelkalk of the Catalan Basin mirrors the palaeobiogeographic distribution at
800 Western Tethys scale. As shown below, the detailed analysis of the occurrence and
801 absence of tetrapod ichnotaxa (Figs. 7, S11, S12, Tables S2, S3) demonstrates that
802 tetrapod ichnofacies can be a useful tool contributing to the understanding of past
803 ecosystems and their evolution (Hunt and Lucas, 2007a, 2007b).

804 Our database of the Middle Triassic tetrapod ichnotaxa and localities all over the
805 world, including the specific time interval and palaeoenvironmental settings (Table S1),
806 shows that the distribution of ichnotaxa appears to be linked to the environmental
807 changes derived from different marine transgressions (Fig. 7) (as reflected in the middle
808 Muschelkalk from the Catalan Basin), being especially notable in the Western Tethys
809 domain (cf. Diedrich, 2002, 2008, 2015; Mujal et al., 2018a). It is important to remark
810 that most of the Middle Triassic tetrapod footprint localities so far known are dated as
811 Anisian, and only a few of them correspond to the Ladinian (Fig. 1; see Table S1 for
812 references). This could be related to the fact that during most part of the Ladinian most
813 of these Triassic basins were under marine settings (e.g., Escudero-Mozo et al., 2015;
814 Franz et al., 2015; Manzanares et al., 2020; and references therein) (Fig. 1). In this
815 sense, successions ranging from the Anisian to the Ladinian, as those from the middle

816 Muschelkalk, give clues to the understanding of the (ichno-) faunal evolution during the
817 Middle Triassic.

818 During the latest Early Triassic (Olenekian) and the early steps of the Middle
819 Triassic (Anisian), the Western Tethys basins were characterised by the presence of
820 archosauromorphs (Mujal et al., 2016b, 2017a). Chirotheriid tracks (and especially
821 *Chirotherium barthii*) and *Rhynchosauroides* are abundant in Spain, France, Morocco,
822 Italy, Switzerland, Germany, Poland, United Kingdom and the USA (see Table S1 for
823 references). Other ichnotaxa are also recorded but not as widely present and abundant as
824 the previous ones (e.g., *Procolophonichnium*, *Chelonipus*, *Isochirotherium*,
825 *Synaptichnium*, and *Rotodactylus*, though the latter may be occasionally abundant).
826 Interestingly, *Chirotherium barthii* and *Rhynchosauroides* are present in further Middle
827 Triassic localities from China (Xing et al., 2013; Xing and Klein, 2019). *C. barthii* is
828 also known from Argentina (Lagnaoui et al., 2019), indicating a virtual global
829 distribution of the corresponding trackmakers.

830 Large-sized tracks referred to chirotheriids are also recorded in some
831 southwestern-southern Gondwanan regions (e.g., Argentina: Marsicano et al., 2004;
832 Melchor and de Valais, 2006; Lagnaoui et al., 2019; Brazil: Leonardi, 1980), including
833 *Chirotherium* and *Isochirotherium*. Therefore, the group of relatively large chirotheriid-
834 trackmakers had already a cosmopolitan distribution during the early stages of the
835 Triassic, as recently shown in the review of the Early Triassic tetrapod fauna by
836 Romano et al. (2020). This is also indicated by the widespread presence across central
837 Pangaea of *Protochirotherium* tracks in the Lower Triassic (Fichter and Kunz, 2004;
838 Klein and Niedźwiedzki, 2012; Klein et al., 2013), which possibly extends back to the
839 upper Permian (Bernardi et al., 2015; Marchetti et al., 2019d). *Rotodactylus* tracks are
840 slightly more abundant in terrestrial palaeoenvironments than in coastal ones (Fig. 7B),
841 which possibly reflect a similar distribution to that of chirotheriid tracks. In fact,
842 chirotheriid and *Rotodactylus* ichnotaxa are commonly found associated (Table S1).

843 Palaeoenvironmental and/or taphonomic biases exist as demonstrated by the
844 poor (or null) ichnological record of non-amniote tetrapods (temnospondyls sensu lato)
845 in the Western Tethys during the Anisian. Only dubious records from few localities of
846 France and Germany are known (Haubold, 1971a; Demathieu and Durand, 1991; Gand
847 et al. 2007). Out from the Western Tethys, potential amphibian tracks are known only
848 from the Moenkopi Formation, USA (Klein and Lucas, 2010a), and New South Wales,
849 Australia (Farman and Bell, 2020) (Table S1). This is in contrast with the important

850 osteological record of Anisian temnospondyls from the Western Tethys (e.g., Spain,
851 Fortuny et al. 2011b; France, Germany and Poland, Schoch and Milner 2000). More
852 recently, Mujal and Schoch (2020) reported temnospondyl tracks from the Ladinian
853 (Lower Keuper) of southern Germany. These authors hypothesised that the lack of
854 record is most probably related to the ecological preferences of temnospondyls, which
855 usually roamed subaquatic settings performing a buoyant/swimming locomotion, hence
856 reducing the preservation potential of footprints.

857 Even if transgressions resulted in different environments across the Western
858 Tethys, basins remained connected during the Middle Triassic as demonstrated by the
859 relatively homogeneous tetrapod ichnoassemblages throughout this domain. With the
860 development of coastal areas, the trackmakers of *Rhynchosauroides* took advantage as
861 reflected by the dominance of this ichnogenus in the Western Tethys coastal
862 palaeoenvironments (Diedrich, 2008; Mujal et al., 2018a). Interestingly,
863 *Procolophonichnium* tracks have a similar palaeoenvironmental distribution to that of
864 *Rhynchosauroides* (Fig. 7), confirming the previous observations of Diedrich (2002) for
865 the Central European Basin. Noteworthy, *Rhynchosauroides* is already abundant in the
866 marginal marine setting of the Arenaria de Val Gardena Formation, from the Lopingian
867 of Italy (Valentini et al., 2007; Marchetti et al., 2019d). This could be indicative of a
868 similar palaeoecology of this older *Rhynchosauroides* morphotype to those of the
869 Middle Triassic; hence further investigations should focus on the comparison of the
870 whole record of this ichnogenus.

871 *Rhynchosauroides* already had a global distribution by the Early and earliest
872 Middle Triassic, being recorded in western and central Europe (Haubold, 1971a, 1971b;
873 Demathieu, 1985; Diedrich, 2002, 2008; Demathieu and Demathieu, 2004; Klein and
874 Niedźwiedzki, 2012; Mujal et al., 2016b, 2017a), western USA (Klein and Lucas,
875 2010a; Lovelace and Lovelace, 2012), Argentina (Melchor and de Valais, 2006) and
876 China (Xing and Klein, 2019). This ichnogenus encompasses a high number of
877 ichnospecies, many of them possibly described from specimens with
878 extramorphological variations (cf. Klein and Niedźwiedzki, 2012); similarly, in several
879 cases *Rhynchosauroides* tracks are usually not identified at the ichnospecies level
880 (Table S1). As a result, this ichnogenus is in need of a comprehensive revision in order
881 to determine its ichnospecific diversity. In any case, certain *Rhynchosauroides*
882 morphotypes are characteristic of specific time intervals and palaeoenvironmental
883 settings: *R. schochardti*, known from the Lower and lowermost Middle Triassic

884 terrestrial settings, and *R. tirolicus* and *R. peabodyi*, known from the Middle Triassic
885 coastal settings of the Western Tethys (Table S1). Therefore, the global distribution of
886 *Rhynchosauroides* during the Early Triassic could be explained by the presence of
887 trackmakers mostly adapted to terrestrial environments. Several of these
888 palaeoenvironments would have evolved to coastal settings during the Middle Triassic,
889 possibly prompting a turnover within the trackmakers of *Rhynchosauroides*. The new
890 trackmakers might have diversified and became dominant due to the expansion of
891 coastal settings. Therefore, there could have been a turnover of faunas from the Early to
892 the Middle Triassic, especially in the Western Tethys, due to the expansion of coastal
893 settings and in detriment of most large archosaurians (see below). Nonetheless, a
894 research bias, with the coastal settings from the Lower Triassic less studied than those
895 of the Middle Triassic, cannot be ruled out.

896 Additionally, tetrapod swimming trace fossils, even if not abundant, are present
897 in all the palaeoenvironments of the Middle Triassic (Fig. 7, Table S1). This could point
898 to a potential taphonomic bias towards the preservation of footprints in environments
899 with a relatively recurrent presence of water. Therefore, such bias could also be applied
900 at a greater scale; this is, there could be a preferential preservation of coastal deposits
901 against more inland ones, and thus the likelihood of finding tetrapod footprints is
902 greater in coastal settings. However, as shown in section 4.3 above, tetrapod track
903 localities of coastal settings are approximately the same as those of alluvial
904 palaeoenvironments (Fig. S11). Regarding the shallow marine settings, a potential
905 research bias is observed, as track localities under this palaeoenvironment are markedly
906 less represented than the other ones (Fig. S11).

907 The potential faunal turnover within the trackmakers of *Rhynchosauroides* can
908 be further explored by analysing the osteological record. Ezcurra and Butler (2015,
909 2018) and Foth et al. (2016) already documented an increase of the morphological
910 disparity of archosauromorphs during the late Early and early Middle Triassic, although
911 the low sampling of Lower Triassic deposits should also be considered (see also Butler
912 et al., 2011; Romano et al., 2020). Ezcurra and Butler (2018), as well as Irmis and
913 Whiteside (2012), suggested that the low rates of diversification within
914 archosauromorphs, but also generally within tetrapods, could be linked to perturbations
915 of the global carbon cycle in the aftermath of the end-Permian mass extinction (for
916 alternative interpretations on the magnitude of the extinction, see Lucas, 2017). The
917 stabilization of the carbon cycle, together with the expansion of coastal settings, would

918 have allowed the diversification of certain tetrapod groups. Interestingly, MacDougall et
919 al. (2019) also documented a turnover within parareptiles during the early steps of the
920 Triassic (see Ruta et al., 2011), showing also a sharp decline during the Middle Triassic;
921 these changes could be linked to the radiation of archosauromorphs. In this sense, the
922 Lower and Middle Triassic tetrapod localities are commonly dominated by
923 archosauromorph faunas (e.g., Pinheiro et al., 2016) and lepidosauromorphs, though the
924 latter being less abundant (e.g., Schoch and Sues, 2018; Simões et al., 2018; Cavvichini
925 et al., 2020; Sobral et al., 2020). Interestingly, the tetrapod tracks apparently mirror such
926 changes, with a high increase and dominance of footprints produced by
927 archosauromorphs (e.g., Mujal et al., 2017a).

928 As observed between the middle Muschelkalk localities of the Catalan Basin,
929 while in Peña Rubí and Pedrera de Can Sallent small-sized footprints are extremely
930 abundant and large ichnotaxa (i.e., chirotheriids) are completely absent, in Puigventós,
931 Montmany and Collcardús chirotheriids are proportionally much more abundant than
932 small-sized taxa (e.g., *Rhynchosauroides*). Interestingly, Peña Rubí and Pedrera de
933 Can Sallent correspond to tidal flat settings, mostly composed of carbonate and very
934 fine- to fine-grained siliciclastic deposits, whereas Puigventós, Montmany and
935 Collcardús correspond to distal alluvial and proximal sabkha settings, mostly composed
936 of fine- to medium-grained siliciclastic deposits. In addition, small ichnotaxa (i.e.,
937 *Rhynchosauroides* among others) are much less abundant than in the tidal (coastal
938 deposits), even if present in these distal alluvial settings (Figs. 7B, 8). The main
939 difference between Peña Rubí and Puigventós and Montmany is the
940 palaeoenvironmental setting, with more terrestrial influence in Puigventós and
941 Montmany than in Peña Rubí (Texts S1 and S3). These considerations can be
942 discussed at Western Tethys (and possibly Pangaeen) level: as recently discussed for the
943 Upper Triassic boreal successions (Klausen et al., 2020), the proliferation of coastal
944 areas, with more marine influence due to the Tethys transgression, may led to the loss of
945 habitats of large archosaur faunas (mostly represented by chirotheriids in the
946 ichnological record). As reflected in the Western Tethys (Table S1), large archosaur
947 ichnofaunas in palaeoenvironments with relatively strong marine influence are
948 persistent and diverse (Fig. 7), though in absolute numbers (e.g., Diedrich, 2008, 2015;
949 Mujal et al., 2018a; Marchetti et al., 2020; Mietto et al., 2020) they are notably less
950 abundant than in terrestrial (alluvial) settings (Figs. 7, 8, Tables S2, S3). This may be
951 further indicative of environmental constraints for large-sized archosaurs as discussed in

952 section 5.1 above. Nonetheless, further quantitative analyses are necessary to untangle
953 the distribution of chirotheriid ichnotaxa.

954 The distribution of Middle Triassic tetrapod ichnotaxa also shows that the distal
955 alluvial and inland settings present a higher (ichno-) diversity than the coastal settings
956 (Figs. 7B, 8, Tables S2, S3). This could respond to the harsher conditions on coastal
957 settings respect to more terrestrial ones. As a result, this could have favoured the
958 proliferation of more generalist taxa (like the potential producers of *Rhynchosauroides*;
959 e.g., Demathieu and Demathieu, 2004; Petti et al., 2013; Mujal et al., 2016b) that better
960 adapted to these environments. In this regard, even without counting the absolute
961 number of footprints of each locality, a reduced tetrapod ichnodiversity is observed in
962 coastal settings, where *Rhynchosauroides* and *Procolophonichnium* tracks dominate
963 (Diedrich, 2008; Mujal et al., 2018a; Marchetti et al., 2020; Mietto et al., 2020). In the
964 same way, as suggested by Marchetti et al. (2020), the proportionally higher number of
965 relatively large archosaur tracks in alluvial settings is probably linked to a different
966 palaeoecology of the trackmakers.

967 We observe that, in fairly age equivalent localities, differences in ichnofaunal
968 composition exist (Fig. 7, Tables S1, S2, S3). Therefore, at the Middle Triassic scale,
969 the presence of certain ichnotaxa is generally more linked to the environmental setting
970 than to the specific age of the deposits. Thus, the temporal evolution of
971 palaeoenvironments may show an (ichno-) faunal replacement, as observed in the Upper
972 Triassic (Stubbs et al., 2013; Bernardi et al., 2018). Further, such environmental
973 constraint would eventually trigger the proliferation of faunas more adapted to the new
974 environments, such as the dinosaur ascendants, which may be poorly represented in the
975 track record before the Ladinian in the Western Tethys (Table S1). In this regard,
976 thorough revisions of ichnotaxa attributed to dinosauromorphs, such as *Rotodactylus*
977 and *Sphingopus* (see Peabody, 1948; Haubold, 1999; Haubold and Klein, 2000, 2002;
978 Brusatte et al., 2011; and Padian, 2013 for alternative interpretations), together with the
979 (so far poor) osteological record, are necessary to provide a wider picture of the
980 temporal range and spatial distribution of the dinosaur lineage. The decline of non-
981 dinosauromorph archosaurs, leading to the dominance of the dinosaur lineage has been
982 recently discussed for the Upper Triassic tetrapod record on the basis of (1)
983 morphological and biomechanical disparity (Stubbs et al., 2013) and (2) the archosaur
984 to dinosaur footprint turnover linked to the Carnian Pluvial Event (Bernardi et al.,
985 2018). During the Middle Triassic, dinosauromorphs were still marginal components of

986 tetrapod ecosystems, becoming significantly more abundant by the end of the Middle
987 Triassic and especially during the Late Triassic. All these observations highlight the
988 necessity of carrying out facies analyses together with ichnological (and generally
989 palaeontological) studies. This is necessary to explore the role that the Middle Triassic
990 environmental changes (linked to marine transgressions) played on the shape of tetrapod
991 ecosystems, including also the radiation of the dinosaur lineage. The expansion of
992 coastal and/or marine influenced environments possibly prompted a regression/decrease
993 of large archosaur faunas (potential producers of chirotheriids), which later evolved to
994 new faunas that took advantage of the new environmental settings (e.g., as represented
995 by the evolutionary novelties present in dinosauromorphs and descendants). It is
996 important to note that, in any case, small-sized neodiapsid faunas (mostly represented
997 by *Rhynchosauroides*) persisted (and expanded) in these coastal/marine influenced
998 environments (Diedrich, 2008; Mujal et al., 2018a, and references therein), though they
999 almost disappeared in the Late Triassic.

1000 In summary, we here suggest a link between the Middle Triassic environmental
1001 changes and the presence and relative abundance of certain (ichno-) faunas (Fig. 13). In
1002 this way, our data permit to distinguish between palaeo(bio)geographic domains of the
1003 Western Tethys: marine influenced ichnoassociations (*Rhynchosauroides*-dominated)
1004 and terrestrial ones (non-*Rhynchosauroides*-dominated). Moreover, in a reverse
1005 analysis, (i) the identification of palaeoenvironments (especially those yielding
1006 *Rhynchosauroides* and Chirotheriidae tracks) and (ii) the age of the successions (i.e.,
1007 Lower or Middle Triassic) might allow to differentiate the potential producers of these
1008 ichnotaxa.

1009

1010 **6. Conclusions**

1011

1012 The Middle Triassic terrestrial record represents an excellent case to study the
1013 tetrapod palaeoecology. This is especially the case of the tetrapod ichnological record,
1014 particularly abundant from this time interval, as ichnites are preserved in the actual
1015 habitats of the corresponding trackmakers. Among the different track localities globally
1016 known (Table S1), those from the middle Muschelkalk successions of the Catalan Basin
1017 are of particular interest. The tracks herein reported, together with those previously
1018 known, reveal a relatively rich ichnodiversity, including: *Procolophonichnium*
1019 *haarmuehlensis*, *Procolophonichnium* isp., *Chelonipus* isp., *Rhynchosauroides tirolicus*,

1020 *Rhynchosauroides* isp., *Rotodactylus* isp., *Chirotherium* cf. *sickleri*, *Chirotherium*
1021 *barthii*, *Isochirotherium* cf. *coureli*, *Sphingopus ferox*, and Chirotheriidae indet. Such
1022 ichnotaxa are widely known among the Western Tethys basins and some
1023 (*Rhynchosauroides* and *C. barthii*) even have a global distribution.

1024 The correlation of each ichnotaxon to its palaeoenvironmental setting, together
1025 with the comparison with further localities, shows that environmental changes (linked to
1026 the Middle Triassic marine transgressions) constrained the distribution of tetrapod
1027 faunas. In the Catalan Basin, the aforementioned ichnotaxa are settled in well-
1028 differentiated ichnoassociations, which are linked to different palaeoenvironments. This
1029 is, tetrapod ichnotaxa are probably controlled by the presence of specific facies.

1030 The most representative ichnotaxon reflecting such constraints is
1031 *Rhynchosauroides*: in coastal palaeoenvironments it is commonly the dominant
1032 ichnotaxon (suggestive of a distinct ichnocoenosis: Diedrich, 2008; Mujal et al., 2018a),
1033 whereas in more inland settings its presence is reduced. Similarly, *Procolophonichnium*
1034 tracks are also more abundant in coastal settings than in alluvial ones. Chirotheriid
1035 footprints show the opposite trend: they are scarce in coastal settings, especially those
1036 built up of fine-grained facies, and commonly dominate in more terrestrial settings.
1037 Therefore, Middle Triassic ichnoassociations are generally either *Rhynchosauroides*-
1038 dominated (coastal settings, especially those with fine-grained facies) or non-
1039 *Rhynchosauroides*-dominated (alluvial settings, even with some marine influence, and
1040 with an increased presence of chirotheriid tracks). Furthermore, tetrapod track diversity
1041 in alluvial settings is notably higher than in coastal settings, suggesting that the
1042 trackmakers of *Rhynchosauroides*, possibly being generalist organisms, took advantage
1043 in coastal palaeoenvironments. This could possibly mirror faunal turnovers during the
1044 Early and Middle Triassic recovery of the ecosystems.

1045 This work highlights the importance of facies analyses when studying tetrapod
1046 ichnofossils. This may result in a better understanding on the presence/absence of
1047 specific ichnotaxa. An integrated sedimentological and ichnological approach sheds
1048 light on the tetrapod palaeobiogeography at the given time interval. In this regard, the
1049 palaeoenvironmental constraints evidenced by the middle Muschelkalk of the Catalan
1050 Basin show the palaeobiogeographic variation of tetrapods of the whole Middle Triassic
1051 Western Tethys, and thus contribute to the understanding of the (ichno-) faunal
1052 responses to environmental change.

1053

1054 **Acknowledgments**

1055 Our special thanks to Belén Muñoz for reporting the discovery of the Puigventós
1056 ichnosite, as well as to Joan Soler for guidance to the outcrops. Manel Méndez, Marc
1057 Riccetto, Alejandro Granados, Montse Vilalta and Albert Vidal are acknowledged for
1058 their fieldwork support and Xènia Aymerich (ICP) for the preparation of the track
1059 samples. We acknowledge Jordi Ibáñez-Insa (GEO3BCN-CSIC, Barcelona) for
1060 mineralogical determinations. C.D.J.S. is granted by a FI AGAUR fellowship (ref. 2020
1061 FI_B 00472) funded by the Secretaria d'Universitats i Recerca de la Generalitat de
1062 Catalunya and the European Social Fund. E.M. acknowledges Secretaria d'Universitats i
1063 Recerca del Departament d'Economia i Coneixement de la Generalitat de Catalunya
1064 (expedient number 2013 CTP 00013) and the Erasmus+ program from the UAB for
1065 funding used for visiting collections at the Institut des Sciences de l'Evolution de
1066 Montpellier (Université Montpellier, France). J.F. is supported by the Spanish Agencia
1067 Estatal de Investigación and the European Regional Development Fund of the European
1068 Union (AEI/FEDER EU, project CGL2017-82654-P). J.F. and O.O. are members of the
1069 consolidated research groups (GRC) 2017 SGR 86 and 1666, respectively, of the
1070 Generalitat de Catalunya. A.B. work is supported by a Juan de la Cierva Incorporación
1071 Fellowship (IJC2018-037685-I, funded by Ministerio de Ciencia e Innovación of the
1072 Spanish Government). We acknowledge support from the CERCA programme (ICP)
1073 from the Generalitat de Catalunya, and the projects “Evolució dels ecosistemes amb
1074 faunes de vertebrats del Permian i el Triàsic de Catalunya” (ref. 2014/100606) and
1075 “Evolució dels ecosistemes durant la transició Paleozoic–Mesozoic a Catalunya” (ref.
1076 CLT009/18/00066), based at the ICP and financially supported by the Departament de
1077 Cultura (Generalitat de Catalunya). We acknowledge the reviewers Lorenzo Marchetti
1078 and Hendrik Klein and the editor Prof. Howard Falcon-Lang, whose comments and
1079 suggestions highly improved a previous version of the manuscript.

1080

1081 **References**

- 1082 Abel. O., 1926. Der erste Fund einer Tetrapodenfährte in den unteren alpinen Trias. Pal.
1083 Z. 7, 22–24.
- 1084 Alroy, J., 2013. Online paleogeographic map generator. <http://paleodb.org/?a=mapForm>
- 1085 Avanzini, M., 2000. *Synaptichnium* tracks with skin impressions from the Anisian
1086 (Middle Triassic) of the Southern Alps (Val di Non – Italy). Ichnos 7(4), 243–251.

- 1087 Avanzini, M., Mietto, P., 2008. Lower and Middle Triassic footprint-based
1088 biochronology in the Italian Southern Alps. *Oryctos* 8, 3–13.
- 1089 Avanzini, M., Renesto, S., 2002. A review of *Rhynchosauroides tirolicus* Abel, 1926
1090 ichnospecies (Middle Triassic: Anisian-Ladinian) and some inferences on
1091 *Rhynchosauroides* trackmaker. *Riv. Ital. Paleontol. S.* 108(1), 51–66.
- 1092 Avanzini, M., Piñuela, L., Garcia-Ramos, J.C., 2010. First report of a Late Jurassic
1093 lizard-like footprint (Asturias, Spain). *J. Iber. Geol.* 36(2), 175–180.
1094 https://doi.org/10.5209/rev_JIGE.2010.v36.n2.5
- 1095 Avanzini, M., Bernardi, M., Nicosia, U., 2011. The Permo-Triassic tetrapod faunal
1096 diversity in the Italian Southern Alps, in: Dar, I.A. (Ed.), *Earth and Environmental*
1097 *Sciences*. InTech, pp. 591–608.
- 1098 Benton, M.J., 2016. The Triassic. *Curr. Biol.* 26, R1205–R1225.
- 1099 Benton, M.J., 2018. Hyperthermal-driven mass extinctions: killing models during the
1100 Permian–Triassic mass extinction. *Phil. Trans. R. Soc. A* 376: 20170076.
1101 <https://doi.org/10.1098/rsta.2017.0076>
- 1102 Benton, M.J., Newell, A.J., 2014. Impacts of global warming on Permo-Triassic
1103 terrestrial ecosystems. *Gondwana Res.* 25, 1308–1337.
1104 <https://doi.org/10.1016/j.gr.2012.12.010>
- 1105 Bernardi, M., Klein, H., Petti, F.M., Ezcurra, M.D., 2015. The origin and early radiation
1106 of archosauriforms: integrating the skeletal and footprint record. *PLoS ONE* 10 (6),
1107 e0128449.
- 1108 Bernardi, M., Gianolla, P., Petti, F.M., Mietto, P., Benton, M.J., 2018. Dinosaur
1109 diversification linked with the Carnian Pluvial Episode. *Nat. Commun.* 9, 1499.
1110 <https://doi.org/10.1038/s41467-018-03996-1>
- 1111 Bernardi, M., Petti, F.M., Simões, T.R., 2019. No longer in the Mesozoic. The Permian
1112 world as a cradle for the origin of key vertebrate groups. *Permophiles* 67, 29–31.
- 1113 Berrocal-Casero, M., Arribas, M., Moratalla, J.J., 2018a. Didactic and divulgative
1114 resources of the Middle Triassic vertebrate Tracksite of Los Arroturos (Province of
1115 Guadalajara, Spain). *Geoheritage* 10, 375–384. [https://doi.org/10.1007/s12371-017-](https://doi.org/10.1007/s12371-017-0244-1)
1116 [0244-1](https://doi.org/10.1007/s12371-017-0244-1)
- 1117 Berrocal-Casero, M., Audije-Gil, J., Castanhinha, R.A., Pérez-Valera J.A., dos Santos,
1118 V. F., Segura M., 2018b. New discoveries of vertebrate remains from the Triassic
1119 of Riba de Santiuste, Guadalajara (Spain). *P. Geologist Assoc.* 129, 526–541.
1120 <https://doi.org/10.1016/j.pgeola.2018.04.009>

- 1121 Bourquin, S., Bercovici, A., López-Gómez, J., Diez, J.B., Broutin, J., Ronchi, A.,
1122 Durand, M., Arche, A., Linol, B., Amour, F., 2011. The Permian-Triassic transition
1123 and the onset of Mesozoic sedimentation at the northwestern peri-Tethyan domain
1124 scale: Palaeogeographic maps and geodynamic implications. *Palaeogeogr.*
1125 *Palaeoclimatol. Palaeoecol.* 299, 265–280.
1126 <https://doi.org/10.1016/j.palaeo.2010.11.007>
- 1127 Brusatte, S. L., Niedźwiedzki, G., and Butler, R. J. 2011. Footprints pull origin and
1128 diversification of dinosaur stem lineage deep into Early Triassic. *Proc. R. Soc. B*
1129 278, 1107–1113. <https://doi.org/10.1098/rspb.2010.1746>
- 1130 Butler, R.J., Brusatte, S.L., Reich, M., Nesbitt, S.J., Schoch, R.R., Hornung, J.J., 2011.
1131 The sail-backed reptile *Ctenosauriscus* from the latest Early Triassic of Germany
1132 and the timing and biogeography of the early archosaur radiation. *PLoS ONE* 6(10),
1133 e25693. <https://doi.org/10.1371/journal.pone.0025693>
- 1134 Calvet, F., Marzo, M., 1994. El Triásico de las Cordilleras Costero Catalanas:
1135 Estratigrafía, Sedimentología y Análisis Secuencial. Cuaderno de Excursión. III
1136 Coloquio de Estratigrafía y Paleostratigrafía del Pérmico y Triásico de España.
1137 Field Guide, 1–53.
- 1138 Calvet, F., Tucker, M.E., Henton, J.M., 1990. Middle Triassic carbonate ramp systems
1139 in the Catalan Basin, northeast Spain: facies, systems tracts, sequences and
1140 controls. *Special Publications International Association of Sedimentology*, 9, 79-
1141 108.
- 1142 Carmona N., Bournod, C., Ponce, J.J., Cuadrado D., 2011. The role of microbial mats in
1143 the preservation of bird footprints: a case study from the mesotidal Bahia Blanca
1144 estuary (Argentina). *SEPM Special Publications* 101, 37–45.
1145 <https://doi.org/10.2110/sepmsp.101.037>
- 1146 Cavicchini, I., Zaher, M., Benton, M.J., 2020. An enigmatic neodiapsid reptile from the
1147 Middle Triassic of England. *J. Vertebr. Paleontol.*, e1781143, 18 pp.
1148 <https://doi.org/10.1080/02724634.2020.1781143>.
- 1149 Cavin, L., Piuze, A., 2020. A Several-Kilometer-Long Archosaur Route in the Triassic of
1150 the Swiss Alps. *Front. Earth Sci.* 8, 4. <https://doi.org/10.3389/feart.2020.00004>
- 1151 Citton, P., Ronchi, A., Nicosia, U., Sacchi, E., Maganuco, S., Cipriani, A., Innamorati,
1152 G., Zuccari, C., Manucci, F., Romano, M., 2020. Tetrapod tracks from the Middle
1153 Triassic of NW Sardinia (Nurra region, Italy). *Ital. J. Geosci.* 139, 309–320.
1154 <https://doi.org/10.3301/IJG.2020.07>

- 1155 Damiani, R., Schoch, R.R., Hellrung, H., Werneburg, R., Gastou, S., 2009. The
1156 plagiosaurid temnospondyl *Plagiosuchus pustuliferus* from the Middle Triassic of
1157 Germany: anatomy and functional morphology of the skull. *Zool. J. Linn. Soc.* 155,
1158 348–373. <https://doi.org/10.1111/j.1096-3642.2008.00444.x>
- 1159 De Jaime-Soguero, C., Mujal, E., Fortuny, J., 2020. First xiphosuran traceway in the
1160 middle Muschelkalk facies (Middle Triassic) of the Catalan Basin (NE Iberian
1161 Peninsula). *Spanish J. Palaentol.* 35 (2), 197–208.
1162 <https://doi.org/10.7203/sjp.35.2.18483>
- 1163 Demathieu, G. 1966. *Rhynchosauroides petri* et *Sphingopus ferox*, nouvelles empreintes
1164 de reptiles des grès Triasiques de la bordure Nord-Est du Massif Central. *C. R.*
1165 *Acad. Sci. Paris D* 263, 483–486.
- 1166 Demathieu, G., 1970. Les empreintes de pas de vertébrés du Trias de la bordure nord-est
1167 du Massif Central. *Cahiers de Paleontologie*, 1–211.
- 1168 Demathieu, G., 1985. Trace fossil assemblages in middle Triassic marginal marine
1169 deposits, Eastern border of the Massif Central, France. In: Curren, H.A. (Ed.),
1170 *Biogenic structures*. SEPM Special Publications 35, 53–66.
- 1171 Demathieu, G., Demathieu, P., 2004. Chirotheria and Other Ichnotaxa of the European
1172 Triassic. *Ichnos* 11(1-2), 79–88. <https://doi.org/10.1080/10420940490444898>
- 1173 Demathieu, G., Durand, M., 1991. Les traces de pas de Tétrapodes dans le Trias
1174 détritique du Car et des Alpes-Maritimes (France). *Bull. Soc. His. Nat. Autun* 32,
1175 4–18.
- 1176 Demathieu, G., Oosterink, H.W., 1983. Die Wirbeltier-Ichnofauna aus dem Unteren
1177 Muschelkalk von Winterswijk (Die Reptilfährten aus der Mitteltrias der
1178 Niederlande). *Staringia* 7, 1–51.
- 1179 Demathieu, G., Oosterink, H.W., 1988. New discoveries of ichnofossils from the
1180 Middle Triassic of Winterswijk (The Netherlands). *Geol. Mijnbouw* 67(1), 3–17.
- 1181 Demathieu, G., Ramos, A., Sopena, A., 1978. Fauna icnológica del Triásico del extremo
1182 noroccidental de la Cordillera Ibérica (Provincia de Guadalajara). *Estud. Geol.* 34,
1183 175–186.
- 1184 Díaz-Martínez, I., Pérez-García, A., 2012. Historical and comparative study of the first
1185 Spanish vertebrate paleoichnological record and bibliographic review of the
1186 Spanish chiroteroiid footprints. *Ichnos* 19, 141–149.
1187 <https://doi.org/10.1080/10420940.2012.685565>

- 1188 Díaz-Martínez, I., Castanera, D., Gasca, J.M., Canudo, J.I., 2015. A reappraisal of the
1189 Middle Triassic chirotheriid *Chirotherium ibericus* Navas, 1906 (Iberian Range NE
1190 Spain), with comments on the Triassic tetrapod track biochronology of the Iberian
1191 Peninsula. *PeerJ* 3, e1044. <https://doi.org/10.7717/peerj.1044>
- 1192 Diedrich, C., 2002. Vertebrate track bed stratigraphy at new megatrack sites in the
1193 Upper Wellenkalk Member and *orbicularis* Member (Muschelkalk, Middle
1194 Triassic) in carbonate tidal flat environments of the western Germanic Basin.
1195 *Palaeogeogr. Palaeoclimatol. Palaeoecol.* 183, 185–208.
1196 [https://doi.org/10.1016/S0031-0182\(01\)00467-9](https://doi.org/10.1016/S0031-0182(01)00467-9)
- 1197 Diedrich, C., 2008. Millions of reptile tracks – Early to Middle Triassic carbonate tidal
1198 flat migration bridges of Central Europe- reptile immigration into the Germanic
1199 Basin. *Palaeogeogr. Palaeoclimatol. Palaeoecol.* 259, 410–423.
1200 <https://doi.org/10.1016/j.palaeo.2007.09.019>
- 1201 Diedrich, C., 2012. Middle Triassic chirotherid trackways on earthquake influenced
1202 intertidal limulid reproduction flats of the European Germanic Basin coasts. *Cent.*
1203 *Eur. J. Geosci.* 4(3), 495–529. <https://doi.org/10.2478/s13533-011-0080-9>
- 1204 Diedrich, C., 2015. *Isochirotherium* trackways, their possible trackmakers
1205 (?*Arizonasaurus*): intercontinental giant archosaur migrations in the Middle
1206 Triassic tsunami-influenced carbonate intertidal mud flats of the European
1207 Germanic Basin. *Carbonates Evaporites* 30, 229–252.
1208 <https://doi.org/10.1007/s13146-014-0228-z>
- 1209 Dinarès-Turell, J., Díez, B.J., Rey, D., Arnal, I., 2005. “Buntsandstein”
1210 magnetostratigraphy and biostratigraphic reappraisal from eastern Iberia: Early and
1211 Middle Triassic stage boundary definitions through correlation to Tethyan sections.
1212 *Palaeogeogr. Palaeoclimatol. Palaeoecol.* 229, 158–77.
1213 <https://doi.org/10.1016/j.palaeo.2005.06.029>
- 1214 Escudero-Mozo, M.J., Márquez-Aliaga, A., Goy, A., Martín-Chivelet, A., López-
1215 Gómez, J., Márquez, L., Arche, A., Plasencia, P., Pla, C., Marzo, M., Sánchez-
1216 Fernández, D. (2015) Middle Triassic carbonate platforms in eastern Iberia:
1217 Evolution of their fauna and palaeogeographic significance in the Western Tethys.
1218 *Palaeogeogr. Palaeoclimatol. Palaeoecol.* 417, 236–260.
1219 <https://doi.org/10.1016/j.palaeo.2014.10.041>
- 1220 Ezcurra, M.D., 2010. Biogeography of Triassic tetrapods: evidence for provincialism
1221 and driven sympatric cladogenesis in the early evolution of modern tetrapod

1222 lineages. *Proc. R. Soc. B* 277(1693), 2547–2552.
1223 <https://doi.org/10.1098/rspb.2010.0508>

1224 Ezcurra, M.D., 2016. The phylogenetic relationships of basal archosauromorphs, with
1225 an emphasis on the systematics of proterosuchian archosauriforms. *PeerJ* 4, e1778.
1226 <https://doi.org/10.7717/peerj.1778>

1227 Ezcurra, M.D., Butler, R.J., 2015. Taxonomy of the proterosuchid archosauriforms
1228 (Diapsida: Archosauromorpha) from the earliest Triassic of South Africa, and
1229 implications for the early archosauriform radiation. *Palaeontology* 58(1), 141–170.
1230 <https://doi.org/10.1111/pala.12130>

1231 Ezcurra, M.D., Butler, R.J., 2018. The rise of the ruling reptiles and ecosystem recovery
1232 from the Permo-Triassic mass extinction. *Proc. R. Soc. B* 285, 20180361.
1233 <https://doi.org/10.1098/rspb.2018.0361>

1234 Falkingham, P.L., 2012. Acquisition of high resolution 3D models using free, open-
1235 source, photogrammetric software. *Paleontol. Electron.* 15, 1–15. [https://doi.org/](https://doi.org/10.26879/264)
1236 [10.26879/264](https://doi.org/10.26879/264)

1237 Falkingham, P.L., 2014. Interpreting ecology and behaviour from the vertebrate fossil
1238 track record. *J. Zool.* 292, 222–228. <https://doi.org/10.1111/jzo.12110>

1239 Farman, R.M., Bell, P.R., 2020. Australia’s earliest tetrapod swimming traces from the
1240 Hawkesbury Sandstone (Middle Triassic) of the Sydney Basin. *J. Paleontol.* 94(5),
1241 966–978. <https://doi.org/10.1017/jpa.2020.22>

1242 Fichter, J., Kunz, R., 2004. New genus and species of chirotheroid tracks in the
1243 Detfurth-Formation (Middle Bunter, Lower Triassic) of Central Germany. *Ichnos*
1244 11, 183–193. <https://doi.org/10.1080/10420940490444997>

1245 Fortuny, J., Bolet, A., Sellés, A.G., Cartanyà, J., Galobart, À., 2011a. New insights on
1246 the Permian and Triassic vertebrates from the Iberian Peninsula with emphasis on
1247 the Pyrenean and Catalanian basins. *J. Iber. Geol.* 37(1), 65–86.
1248 https://doi.org/10.5209/rev_JIGE.2011.v37.n1.5

1249 Fortuny, J., Galobart, À., De Santisteban, C., 2011b. A new capitosaur from the Middle
1250 Triassic of Spain and the relationships within the Capitosauria. *Acta Palaeontol.*
1251 *Pol.* 56(3), 553–566. <https://doi.org/10.4202/app.2010.0025>

1252 Foth, C., Ezcurra, M.D., Sookias, R.B., Brusatte, S.L., Butler, R.J., 2016. Unappreciated
1253 diversification of stem archosaurs during the Middle Triassic predated the
1254 dominance of dinosaurs. *BMC Evol. Biol.* 16, 188. [https://doi.org/10.1186/s12862-](https://doi.org/10.1186/s12862-016-0761-6)
1255 [016-0761-6](https://doi.org/10.1186/s12862-016-0761-6)

- 1256 Franz, M., Henniger, M., Barnasch, J., 2013. The strong diachronous
1257 Muschelkalk/Keuper facies shift in the Central European Basin: implications from
1258 the type-section of the Erfurt Formation (Lower Keuper, Triassic) and basin-wide
1259 correlations. *Int. J. Earth Sci.* 102, 761–780. [https://doi.org/10.1007/s00531-012-](https://doi.org/10.1007/s00531-012-0823-y)
1260 0823-y
- 1261 Franz, M., Kaiser, S.I., Fischer, J., Heunisch, C., Kustatscher, E., Luppold, F.W.,
1262 Berner, U., Röhlings, H.G., 2015. Eustatic and climatic control on the Upper
1263 Muschelkalk Sea (late Anisian/Ladinian) in the Central European Basin. *Global*
1264 *Planet. Change* 135, 1–27. <https://doi.org/10.1016/j.gloplacha.2015.09.014>
- 1265 Galán-Abellán, B., López-Gómez, J., Barrenechea, J.F., Marzo, M., De la Horra, R.,
1266 Arche, A., 2013. The beginning of the Buntsandstein cycle (Early-Middle Triassic)
1267 in the Catalan Ranges, NE Spain: Sedimentary and palaeogeographic implications.
1268 *Sediment. Geol.* 296, 86–102. <https://doi.org/10.1016/j.sedgeo.2013.08.006>
- 1269 Gand, G., Demathieu, G., Montenat, C., 2007. Les traces de pas d'amphibiens, de
1270 dinosaures et autres reptiles du Mésozoïque français: Inventaire et interprétations.
1271 *Palaeovertebrata* 35(1–4), 1–149. <https://doi.org/10.18563/pv.35.1-4.1-149>
- 1272 Gand, G., De La Horra, R., Galán-Abellán, B., López-Gómez, J., Barrenechea, J. F.,
1273 Arche, A., Benito, I., 2010. New ichnites from the Middle Triassic of the Iberian
1274 Ranges (Spain): paleoenvironmental and paleogeographical implications. *Hist.*
1275 *Biol.* 22(1–3), 40–56. <https://doi.org/10.1080/08912961003644096>
- 1276 Haubold, H., 1967. Eine Pseudosuchier-Fährtenfauna aus dem Buntsandstein
1277 Südthüringens. *Hallesches Jb. mitteldt. Erdgesch.* 8, 12–48.
- 1278 Haubold, H., 1971a. *Ichnia Amphibiorum et Reptiliorum fossilium*. *Encyclopedia of*
1279 *Paleoherpetology*, 18. Gustav Fischer Verlag, Stuttgart, Germany, and Portland,
1280 USA.
- 1281 Haubold, H., 1971b. Die Tetrapodenfährten des Buntsandsteins in der Deutschen
1282 Demokratischen Republik und in Westdeutschland und ihre Äquivalente in der
1283 gesamten Trias. *Paläontologische Abhandlungen, Abteilung A Paläozoologie*, 395–
1284 548.
- 1285 Haubold, H., 1984. *Saurierfährten* (2nd ed.). Die Neue Brehm-Bucherei 479,
1286 Wittenberg (Ziemsen).
- 1287 Haubold, H., 1999. Tracks of the Dinosauromorpha from the Early Triassic, in
1288 Bachmann, G.H., Lerche, I. (Eds.), *Triassic. Zentralbl. Geol. Paläont., Teil I*, 1998
1289 (7–8), Stuttgart, pp. 783–795.

- 1290 Haubold, H., 2006. Die Saurierfährten *Chirotherium barthii* Kaup, 1835 – das
1291 Typusmaterial aus dem Buntsandstein bei Hildburghausen/Thüringen und das
1292 *Chirotherium*-Monument. Veröffentlichungen Naturhist. Museum Schleusingen
1293 21, 3–31.
- 1294 Haubold, H., Klein, H., 2000. Die dinosauroiden Fährten *Parachirotherium*-*Atreipus*-
1295 *Grallator* aus dem unteren Mittelkeuper (Obere Trias: Ladin, Karn, ?Nor) in
1296 Franken: Hallesches Jahrb. Geowiss. B 22, 59–85.
- 1297 Haubold, H., Klein, H., 2002. Chirotherien und Grallatoriden aus der Unteren bis
1298 Oberen Trias Mitteleuropas und die Entstehung der Dinosauria. Hallesches Jahrb.
1299 Geowiss. B 24, 1–22.
- 1300 Holst, H.K.H., Smit, J., Veenstra, E., 1970. Lacertoid footprints from the Early Middle
1301 Triassic at Haarmuhle, near Altstette, W. Germany. Proc. K. Ned. Akad. van Wet.
1302 B 73(2), 157–165.
- 1303 Hunt, A.P., Lucas, S.G., 2007a. Tetrapod ichnofacies: a new paradigm. Ichnos 14, 59–
1304 68. <https://doi.org/10.1080/10420940601006826>
- 1305 Hunt, A.P., Lucas, S.G., 2007b. The Triassic tetrapod track record: Ichnofaunas,
1306 ichnofacies and biochronology. N. M. Mus. Nat. Hist. Sci. Bull. 41, 78–87.
- 1307 Irmis, R.B., Whiteside, J.H., 2012. Delayed recovery of non-marine tetrapods after the
1308 end-Permian mass extinction tracks global carbon cycle. Proc. R. Soc. B 279,
1309 1310–1318. <https://doi.org/10.1098/rspb.2011.1895>
- 1310 Klausen, T.G., Paterson, N.W., Benton, M.J., 2020. Geological control on dinosaurs’
1311 rise to dominance: Late Triassic ecosystem stress by relative sea level change.
1312 Terra Nova. <https://doi.org/10.1111/TER.12480>
- 1313 Kaup, J.J., 1835. Fährten von Beuteltieren. Das Tierreich, 246–248.
- 1314 Klein, H., Haubold, H., 2003. Differenzierung von ausgewählten Chirotherien der Trias
1315 mittels Landmarkanalyse. Hallesches Jahrb. Geowiss. B 25, 21–36.
- 1316 Klein, H., Haubold, H., 2007. Archosaur footprints –potential for biochronology of
1317 Triassic continental sequences, in: Lucas, S.G., Spielmann, J.A. (Eds.), The Global
1318 Triassic. N. M. Mus. Nat. Hist. Sci. Bull. 41, 120–130.
- 1319 Klein, H., Lucas, S.G., 2010a. Review of the tetrapod ichnofauna of the Moenkopi
1320 Formation/group (Early-Middle Triassic) of the American Southwest. N. M. Mus.
1321 Nat. Hist. Sci. Bull. 50, 1–67.

- 1322 Klein, H., Lucas, S.G., 2010b. Tetrapod footprints – their use in biostratigraphy and
 1323 biochronology of the Triassic. *Geol. Soc. Lond., Spec. Publ.* 334, 419–446.
 1324 <https://doi.org/10.1144/SP334.14>
- 1325 Klein, H., Lucas, S.G., 2018. Diverse Middle Triassic tetrapod footprints assemblage
 1326 from the Muschelkalk of Germany. *Ichnos* 25, 162–176.
 1327 <https://doi.org/10.1080/10420940.2017.1337632>
- 1328 Klein, H., Niedźwiedzki, G., 2012. Revision of the Lower Triassic tetrapod ichnofauna
 1329 from Wióry, Holy Cross Mountains, Poland. *N. M. Mus. Nat. Hist. Sci. Bull.* 56, 1–
 1330 62.
- 1331 Klein, H., Voigt, S., Saber, H., Schneider, J.W., Hminna, A., Fischer, J., Lagnaoui A.,
 1332 Brosig, A., 2011. First occurrence of a Middle Triassic tetrapod ichnofauna from
 1333 the Argana Basin (Western High Atlas, Morocco). *Palaeogeogr. Palaeoclimatol.*
 1334 *Palaeoecol.* 307, 218–231. <https://doi.org/10.1016/j.palaeo.2011.05.021>
- 1335 Klein, H., Niedźwiedzki, G., Voigt, S., Lagnaoui, A., Hminna, A., Saber, H., Schneider,
 1336 J.W., 2013. The tetrapod ichnogenus *Protochirotherium* Fichter and Kunz 2004, a
 1337 characteristic Early Triassic morphotype of Central Pangea. *Ichnos* 20, 24–30.
 1338 <https://doi.org/10.1080/10420940.2012.757699>
- 1339 Klein, H., Lucas, S.G., Voigt, S., 2015. Revision of the Permian-Triassic Tetrapod
 1340 Ichnogenus *Procolophonichnium* Nopcsa 1923 with description of the new
 1341 ichnospecies *P. lockleyi*. *Ichnos* 22(3-4), 155–176.
 1342 <https://doi.org/10.1080/10420940.2015.1063490>
- 1343 Klein, H., Wizevich, M.C., Thüring, B., Marty, D., Thüring, S., Falkingham, P., Meyer,
 1344 C.A., 2016. Triassic chirotheriid footprints from the Swiss Alps: ichnotaxonomy
 1345 and depositional environment (Cantons Wallis & Glarus). *Swiss J. Palaeontol.*
 1346 135(2), 295–314. <https://doi.org/10.1007/s13358-016-0119-0>
- 1347 Kotański, Z., Gierliński, G., Ptaszyński, T., 2004. Reptile tracks (*Rotodactylus*) from the
 1348 Middle Triassic of the Djurdjura Mountains in Algeria. *Geol. Q.* 48(1), 89–96.
- 1349 Lagnaoui, A., Melchor, R.N., Bellosi, E., Villegas, P., 2019. Middle Triassic
 1350 *Pentasauropus*-dominated ichnofauna from the western Gondwana:
 1351 Ichnotaxonomy, palaeoenvironment, biostratigraphy and palaeobiogeography.
 1352 *Palaeogeogr. Palaeoclimatol. Palaeoecol.* 524, 41–61.
 1353 <https://doi.org/10.1016/j.palaeo.2019.03.020>

- 1354 Leonardi, G., 1980. *Isochirotherium* sp.: pista de um gigantesco tecodonte na Formação
1355 Antenor Navarro (Triássico), Sousa, Paraíba, Brasil. Revista Brasileira de
1356 Geociências 10, 186–190.
- 1357 Leonardi, G., 1987. Glossary and Manual of Tetrapod Footprint Palaeoichnology.
1358 Departamento Nacional de Produção Mineral, Brasília.
- 1359 Lichtig, A.J., Lucas, S.G., Klein, H., Lovelace, D.M., 2018. Triassic turtle tracks and
1360 the origin of turtles. Hist. Biol. 30 (8), 1112–1122.
1361 <https://doi.org/10.1080/08912963.2017.1339037>
- 1362 López-Gómez, J., Arche, A., Pérez-López, A., 2002. Permian and Triassic, in: Gibbons,
1363 W., Moreno, M.T. (Eds.), The Geology of Spain. Geological Society of London,
1364 London, pp. 185–212.
- 1365 Lovelace, D.M., Lovelace, S.D., 2012. Paleoenvironments and paleoecology of a Lower
1366 Triassic invertebrate and vertebrate ichnoassemblage from the Red Peak Formation
1367 (Chugwater Group), Central Wyoming. Palaios 27, 636–657. [https://doi.org/](https://doi.org/10.2307/23362122)
1368 [10.2307/23362122](https://doi.org/10.2307/23362122)
- 1369 Lucas, S.G., 2010. The Triassic timescale based on nonmarine tetrapod biostratigraphy
1370 and biochronology. Geological Society, London, Special Publications 334, 447–
1371 500. <https://doi.org/10.1144/SP334.15>
- 1372 Lucas, S.G., 2017. Permian tetrapod extinction events. Earth-Sci. Rev. 170, 31–60.
1373 <https://doi.org/10.1016/j.earscirev.2017.04.008>
- 1374 Lucas S.G., 2018. Permian tetrapod biochronology, correlation and evolutionary events.
1375 Geological Society, London, Special Publications 450, 405–444.
1376 <https://doi.org/10.1144/SP450.12>
- 1377 Lucas, S.G., 2019. An ichnological perspective on some major events of Paleozoic
1378 tetrapod evolution. Boll. Soc. Paleont. Ital. 58(3), 223–266.
1379 <https://doi.org/10.4435/BSPI.2019.20>
- 1380 MacDougall, M.J., Brocklehurst, N., Fröbisch, J., 2019. Species richness and disparity
1381 of parareptiles across the end-Permian mass extinction. Proc. R. Soc. B 286,
1382 20182572. <https://doi.org/10.1098/rspb.2018.2572>
- 1383 Maidwell F., 1911. Notes on footprints from the Keuper of Runcorn Hill. Liverpool
1384 Geological Society 11, 140–152.
- 1385 Mallison, H., Wings, O., 2014. Photogrammetry in Paleontology, a practical guide. J.
1386 Paleontol. Tech. 12, 1–31.

- 1387 Manzanares, E., Escudero-Mozo, M.J., Ferrón, H., Martínez-Pérez, C., Botella, H.,
1388 2020. Middle Triassic sharks from the Catalan Coastal ranges (NE Spain) and
1389 faunal colonization patterns during the westward transgression of Tethys.
1390 *Palaeogeogr. Palaeoclimatol. Palaeoecol.* 539, 109489.
1391 <https://doi.org/10.1016/j.palaeo.2019.109489>
- 1392 Marchetti, L., Tessarollo, A., Felletti, F., Ronchi, A., 2017. Tetrapod footprint
1393 paleoecology: behavior, taphonomy and ichnofauna disentangled. A case study
1394 from the Lower Permian of the Southern Alps (Italy). *Palaios* 32, 506–527.
1395 <https://doi.org/10.2110/palo.2016.108>
- 1396 Marchetti, L., Belvedere, M., Voigt, V., Klein, H., Castanera, D., Díaz-Martínez, I.,
1397 Marty, D., Xing, L., Feola, S., Melchor, R.N., Farlow, J.O., 2019b. Defining the
1398 morphological quality of fossil footprints. Problems and principles of preservation
1399 in tetrapod ichnology with examples from the Palaeozoic to the present. *Earth-Sci.*
1400 *Rev.* 193, 109–145. <https://doi.org/10.1016/j.earscirev.2019.04.008>
- 1401 Marchetti, L., Van Der Donck, H., Van Hylckama Vlieg, M., During, M.A.D., 2019c.
1402 Leaving only trace fossils - the unknown visitors of Winterswijk. *Grondboor &*
1403 *Hamer, Staringia* 16, 250–257.
- 1404 Marchetti, L., Voigt, S., Klein, H., 2019d. Revision of Late Permian tetrapod tracks
1405 from the Dolomites (Trentino-Alto Adige, Italy). *Hist. Biol.* 31(6), 748–783.
1406 <https://doi.org/10.1080/08912963.2017.1391806>
- 1407 Marchetti, L., Voigt, S., Lucas, S.G., Francischini, H., Dentzien-Dias, P., Sacchi, R.,
1408 Mangiacotti, M., Scali, S., Gazzola, A., Ronchi, A., Millhouse, A. 2019a. Tetrapod
1409 ichnotaxonomy in eolian paleoenvironments (Coconino and De Chelly formations,
1410 Arizona) and late Cisuralian (Permian) sauropsid radiation. *Earth-Sci. Rev.* 190,
1411 148–170. <https://doi.org/10.1016/j.earscirev.2018.12.011>
- 1412 Marchetti, L., Klein, H., Falk, D., Wings, O., 2020. *Synaptichnium* tracks from the
1413 Middle Muschelkalk (Middle Triassic, Anisian) Bernburg site (Saxony-Anhalt,
1414 Germany). *Ann. Soc. Geol. Pol.* 90, 12 pp. <https://doi.org/10.14241/asgp.2020.12>
- 1415 Maron, M., Muttoni, G., Rigo, M., Gianolla, P., Kent, D.V., 2019. New
1416 magnetobiostratigraphic results from the Ladinian of the Dolomites and
1417 implications for the Triassic geomagnetic polarity timescale. *Palaeogeogr.*
1418 *Palaeoclimatol. Palaeoecol.* 517, 52–73.
1419 <https://doi.org/10.1016/j.palaeo.2018.11.024>

- 1420 Márquez-Aliaga, A., Valenzuela-Rios, J.I., Calvet, F., Budurov, K., 2000. Middle
1421 Triassic conodonts from northeastern Spain; biostratigraphic implications. *Terra*
1422 *Nova* 12, 77–83.
- 1423 Marsicano, C.A., Arcuci, A.B., Mancuso, A.C., Caselli, A.T., 2004. Middle Triassic
1424 tetrapod footprints of southern South America. *Ameghiniana* 41(2), 171–184.
- 1425 Marsicano, C.A., Wilson, J.A., Smith, R.M.H., 2014. A temnospondyl trackway from
1426 the early Mesozoic of Western Gondwana and its implications for basal tetrapod
1427 locomotion. *PLoS ONE* 9, e103255. <https://doi.org/10.1371/journal.pone.0103255>
- 1428 Marty, D., Strasser, A., Meyer, C.A., 2009. Formation and Taphonomy of Human
1429 Footprints in Microbial Mats of Present-Day Tidal-flat Environments: Implications
1430 for the Study of Fossil Footprints. *Ichnos* 16(1–2), 127–142.
1431 <https://doi.org/10.1080/10420940802471027>
- 1432 Marzo, M., 1980. El Buntsandstein de las Catalánides: estratigrafía y procesos de
1433 sedimentación. [PhD Tesis], 1–634.
- 1434 Melchor, R.N., 2015. Application of vertebrate trace fossils to paleoenvironmental
1435 analysis. *Palaeogeogr. Palaeoclimatol. Palaeoecol.* 439, 79–96.
1436 <https://doi.org/10.1016/j.palaeo.2015.03.028>.
- 1437 Melchor, R. N., Sarjeant, W.A.S., 2004. Small amphibian and reptile footprints from the
1438 Permian Carapacha Basin, Argentina. *Ichnos* 11, 57–78.
1439 <https://doi.org/10.1080/10420940490428814>.
- 1440 Melchor, R. N., De Valais, S., 2006. A review of Triassic tetrapod track assemblages
1441 from Argentina. *Palaeontology* 49, 355–379. [https://doi.org/10.1111/j.1475-](https://doi.org/10.1111/j.1475-4983.2006.00538.x)
1442 [4983.2006.00538.x](https://doi.org/10.1111/j.1475-4983.2006.00538.x)
- 1443 Mietto, P., Avanzini, M., Belvedere, M., Bernardi, M., Dalla Vecchia, F.M., D'Orazi
1444 Porchetti, S., Gianolla, P., Petti, F.M., 2020. Triassic tetrapod ichnofossils from
1445 Italy: the state of the art, in: Romano, M., Citton, P. (Eds.), *Tetrapod ichnology in*
1446 *Italy: the state of the art. J. Med. Earth Sci.* 12, 83–136.
1447 <https://doi.org/10.3304/jmes.2020.17066>
- 1448 Morad, S., Al-Aasm, I.S., Longstaffe, F.J., Marfil, R., De Ros, L. F., Johansen, H.,
1449 Marzo, M., 1995. Diagenesis of a mixed siliciclastic/evaporitic sequence of the
1450 Middle Muschelkalk (Middle Triassic), the Catalan Coastal Range, NE Spain.
1451 *Sedimentology* 42, 749–768. <https://doi.org/10.1111/j.1365-3091.1995.tb00407.x>
- 1452 Mujal, E., Schoch, R.R., 2020. Middle Triassic (Ladinian) amphibian tracks from the
1453 Lower Keuper succession of southern Germany: Implications for temnospondyl

1454 locomotion and track preservation. *Palaeogeogr. Palaeoclimatol. Palaeoecol.* 543,
1455 109625. <https://doi.org/10.1016/j.palaeo.2020.109625>

1456 Mujal, E., Fortuny, J., Rodríguez-Salgado, P., Diviu, M., Oms, O., Galobart, À., 2015.
1457 First footprints occurrence from the Muschelkalk detrital unit of the Catalan
1458 Basin: 3D analyses and paleoichnological implications. *Spanish J. Palaentol.* 30,
1459 97–107. <https://doi.org/10.7203/sjp.30.1.17204>

1460 Mujal, E., Fortuny, J., Oms, O., Bolet, A., Galobart, À., Anadón, P., 2016a.
1461 Palaeoenvironmental reconstruction of an Early Permian ichnoassemblage from the
1462 NE Iberian Peninsula (Pyrenean Basin). *Geol. Mag.* 153 (4), 578–600.
1463 <https://doi.org/10.1017/S0016756815000576>

1464 Mujal, E., Gretter, N., Ronchi, A., López-Gómez, J., Falconnet, J., Diez, J.B., De la
1465 Horra, R., Bolet, A., Oms, O., Arche, A., Barrenechea, JF., Steyer, J-S., Fortuny, J.,
1466 2016b. Constraining the Permian/Triassic boundary in continental environments:
1467 stratigraphic and paleontological record from the Southern-Eastern Pyrenees (NE
1468 Iberian Peninsula). *Palaeogeogr. Palaeoclimatol. Palaeoecol.* 445, 18–37.
1469 <https://doi.org/10.1016/j.palaeo.2015.12.008>

1470 Mujal, E., Fortuny, J., Bolet, A., Oms, O., López, J.Á., 2017a. An archosauromorph
1471 dominated ichnoassemblage in fluvial settings from the late Early Triassic of the
1472 Catalan Pyrenees (NE Iberian Peninsula). *Plos ONE* 12(4), e0174693.
1473 <https://doi.org/10.1371/journal.pone.0174693>

1474 Mujal, E., Fortuny, J., Pérez-Cano, J., Dinarès-Turell, J., Ibáñez-Insa, J., Oms, O., Vila,
1475 I., Bolet, A., Anadón, P., 2017b. Integrated multi-stratigraphic study of the Coll de
1476 Terrers late Permian-Early Triassic continental succession from the Catalan
1477 Pyrenees (NE Iberian Peninsula): A geologic reference record for equatorial
1478 Pangaea. *Global Planet. Change* 159, 46–60.
1479 <https://doi.org/10.1016/j.gloplacha.2017.10.004>

1480 Mujal, E., Belaústegui, Z., Fortuny, J., Bolet, A., Oms, O., López, J.Á., 2018b.
1481 Ichnological evidence of a horseshoe crab hot-spot in the Early Triassic
1482 Buntsandstein continental deposits from the Catalan Pyrenees (NE Iberian
1483 Peninsula). *J. Iber. Geol.* 44, 139–153. <https://doi.org/10.1007/s41513-017-0026-2>

1484 Mujal, E., Iglesias, G., Oms, O., Fortuny, J., Bolet, A., Méndez, J.M., 2018a.
1485 *Rhynchosauroides* footprint variability in a Muschelkalk detrital interval late
1486 Anisian-middle Ladinian) from the Catalan Basin (NE Iberian Peninsula). *Ichnos*
1487 25(2–3), 150–161. <https://doi.org/10.1080/10420940.2017.1337571>

- 1488 Mujal, E., Marchetti, L., Schoch, R.R., Fortuny, J., 2020. Upper Paleozoic to lower
1489 Mesozoic tetrapod ichnology revisited: Photogrammetry and relative depth pattern
1490 inferences on functional prevalence of autopodial. *Front. Earth Sci.* 8, 248.
1491 <https://doi.org/10.3389/feart.2020.00248>
- 1492 Niedźwiedzki, G., Brusatte, S.L., Butler, R.J., 2013. *Prorotodactylus* and *Rotodactylus*
1493 tracks: an ichnological record of dinosauromorphs from the Early–Middle Triassic
1494 of Poland, in: Nesbit, S.J., Desojo, J.B., Irmis, R.B. (Eds.), *Anatomy, Phylogeny
1495 and Palaeobiology of Early Archosaurs and their Kin*. Geological Society Special
1496 Publications 379. Geological Society of London, London, pp. 319–351.
- 1497 Niedźwiedzki, G., Soussi, M., Boukhalfa, K., Gierliński, G.D., 2017. Middle-Upper
1498 Triassic and Middle Jurassic tetrapod track assemblages of Southern Tunisia,
1499 Sahara Platform. *J. Afr. Earth Sci.* 129, 31–44.
1500 <https://doi.org/10.1016/j.jafrearsci.2016.12.006>
- 1501 Nopcsa, F.v., 1923. Die Familien der Reptilien. *Fortsch. Geol. Paläont.* 2, 210.
- 1502 Ortí, F., Pérez-López, A., Salvany, J.M., 2017. Triassic evaporites of Iberia:
1503 sedimentologic and palaeogeographic implications for the western Neotethys
1504 evolution during the Middle Triassic–Earliest Jurassic. *Palaeogeogr. Palaeoclimatol.
1505 Palaeoecol.* 471, 157–180. <https://doi.org/10.1016/j.palaeo.2017.01.025>
- 1506 Ortí, F., Salvany, J.M., Rosell, L., Castelltort, X., Inglès, M., Playà, E., 2018. Middle
1507 Triassic evaporite sedimentation in the Catalan basin: implications for the
1508 paleogeographic evolution in the NE Iberian platform. *Sediment. Geol.* 374, 158–
1509 178. <https://doi.org/10.1016/j.sedgeo.2018.07.005>
- 1510 Padian, K., 2013. The problem of dinosaur origins: integrating three approaches to the
1511 rise of Dinosauria. *Earth Environ. Sci. Trans. R. Soc. Edinb.* 103, 1–20.
- 1512 Peabody, F.E., 1948. Reptile and amphibian trackways from the Moenkopi Formation
1513 of
1514 Arizona and Utah. *Univ. Calif. Publ. Bull. Dep. Geol. Sci.* 27, 295–468.
- 1515 Pérez-López A., 1993. Estudio de las huellas de reptil, del icnogénero
1516 *Brachychirotherium*, encontradas en el Triásico subbético de Cambil (Jaén). *Estud.
1517 Geol.* 49, 77–83. <https://doi.org/10.3989/egeol.93491-2340>
- 1518 Petti F.M., Bernardi M., Kustatscher E., Renesto S., Avanzini M., 2013. Diversity of
1519 continental tetrapods and plants in the Triassic of the Southern Alps: Ichnological,
1520 Paleozoological and Paleobotanical evidence, in: Tanner L.H., Spielmann J.A.,

- 1521 Lucas S.G. (Eds.), The Triassic System. N. M. Mus. Nat. Hist. Sci. Bull. 61, pp.
1522 458–484.
- 1523 Pinheiro, F.L., França, M.A.G., Lacerda, M.B., Butler, R.J., Schultz, C.L., 2016. An
1524 exceptional fossil skull from South America and the origins of the archosauriform
1525 radiation. Sci. Rep. 6, 22817. <https://doi.org/10.1038/srep22817>
- 1526 Reolid, J., Reolid, M., 2017. Traces of Floating Archosaurs: An Interpretation of the
1527 enigmatic trace fossils from the Triassic of the Tabular Cover o Southern Spain,
1528 Ichnos 24(3), 222–233. <https://doi.org/10.1080/10420940.2016.1265524>
- 1529 Reolid, M., Márquez-Aliaga, A., Belinchón, M., García-Fórner, A., Villena, J.,
1530 Martínez-Pérez, C., 2018. Ichnological evidence of semi-aquatic locomotion in
1531 early turtles from Eastern Iberia during the Carnian Humid Episode (Late Triassic).
1532 Palaeogeogr. Palaeoclimatol. Palaeoecol. 490, 450–461.
1533 <https://doi.org/10.1016/j.palaeo.2017.11.025>
- 1534 Reolid, J., Cardenal, F.J., Reolid, M., Mata, E., 2020. 3D Imaging of southernmost
1535 Triassic archosaur footprints from Europe (Southern Spain). J. Iber. Geol. 46, 145–
1536 161. <https://doi.org/10.1007/s41513-020-00125-0>
- 1537 Rieppel, O., Hagdorn, H., 1998. Fossil reptiles from the Spanish Muschelkalk (Mont-ral
1538 and Alcover, Province Tarragona). Hist. Biol. 13(1), 77–97.
1539 <https://doi.org/10.1080/08912969809386575>
- 1540 Rieppel, O., 2000. Sauropterygia I: Placodontia, Pachypleurosauria, Nothosauroida,
1541 Pistosauroida. In P. Wellnhofer (Ed.), Handbuch der Paläoherpetologie, Teil 12A.
1542 Verlag Dr. Friedrich Pfeil, Munich, pp. 134.
- 1543 Romano, M., Bernardi, M., Petti, F.M., Rubidge, B., Hancox, J., Benton, M.J., 2020.
1544 Early Triassic terrestrial tetrapod faune: a review. Earth-Sci. Rev. 210, 103331.
1545 <https://doi.org/10.1016/j.earscirev.2020.103331>
- 1546 Rühle v. Lilienstern, H., 1939. Fährten und Spuren im *Chirotherium*-Sandstein von
1547 Südthüringen. Fortschritte der Geologie und Paläontologie 12(40), 293–387.
- 1548 Ruta, M., Cisneros, J.C., Liebrecht, T., Tsuji, L.A., Müller J., 2011. Amniotes through
1549 major biological crises: faunal turnover among Parareptiles and the end-Permian
1550 mass extinction. Palaeontology 54(5), 1117–1137. <https://doi.org/10.1111/j.1475-4983.2011.01051.x>
- 1552 Schneider, J.W., Lucas, S.G., Scholze, F., Voigt, S., Marchetti, L., Klein, H., Opluštil,
1553 S., Wernerburg, R., Golubevm, V.K., Barrick, J.E., Nemyrovska, T., Ronchi, A.,
1554 Day, M.O., Silantiev, V.V., Rößler, R., Saber, H., Linnemann, U., Zharinova, V.,

1555 Shen, S.-Z., 2020. Late Paleozoic–early Mesozoic continental biostratigraphy—
1556 Links to the Standard Global Chronostratigraphic Scale. *Palaeoworld*, 29(2), 186–
1557 238. <https://doi.org/10.1016/j.palwor.2019.09.001>.

1558 Schoch, R.R., Milner, A.R., 2000. *Handbuch der Paläoherpetologie 3B:*
1559 *Stereospondyli*. Pfeil, Munich, 203 pp.

1560 Schoch, R.R., Seegis, D., 2016. A Middle Triassic palaeontological gold mine: the
1561 vertebrate deposits of Vellberg (Germany). *Palaeogeogr. Palaeoclimatol.*
1562 *Palaeoecol.* 459, 249–267. <https://doi.org/10.1016/j.palaeo.2016.07.002>

1563 Schoch, R., Sues, H.-D., 2015. A Middle Triassic stem-turtle and the evolution of the
1564 turtle body plan. *Nature* 523, 584–587. <https://doi.org/10.1038/nature14472>

1565 Schoch, R.R., Sues, H.-D., 2018. A new lepidosauromorph reptile from the Middle
1566 Triassic (Ladinian) of Germany and its phylogenetic relationships. *J. Syst.*
1567 *Palaeontol.* 12, 113–131. <https://doi.org/10.1080/02724634.2018.1444619>

1568 Schoch, R.R., Ullmann, F., Rozynek, B., Ziegler, R., Seegis, D., Sues, H.-D.,
1569 2018. Tetrapod diversity and palaeoecology in the German Middle Triassic (Lower
1570 Keuper) documented by tooth morphotypes. *Palaeobio. Palaeoenv.* 98, 615–638.
1571 <https://doi.org/10.1007/s12549-018-0327-2>

1572 Simões, T.R., Caldwell, M.W., Tałanda, M., Bernardi, M., Palci, A., Vernygora, O.,
1573 Bernardini, F. Marcini, L., Nydam, R., 2018. The origin of squamates revealed by a
1574 Middle Triassic lizard from the Italian Alps. *Nature* 557, 706–709.
1575 <https://doi.org/10.1038/s41586-018-0093-3>

1576 Sobral, G., Simões, T.R., Schoch, R.R., 2020. A tiny new Middle Triassic stem-
1577 lepidosauromorph from Germany: implications for the early evolution of
1578 lepidosauromorphs and the Vellberg fauna. *Sci. Rep.* 10, 2273.
1579 <https://doi.org/10.1038/s41598-020-58883-x>

1580 Solé de Porta, N., Calvet, F., Torrento, L., 1987. Análisis palinológico del Triásico de
1581 los Catalanides (NE España). *Cuad. Geol. Ibér.* 11, 237–254.

1582 Stubbs, T.L., Pierce, S.E., Rayfield, E.J., Anderson, P.S.L., 2013. Morphological and
1583 biomechanical disparity of crocodile-line archosaurs following the end-Triassic
1584 extinction. *Proc. R. Soc. B.* 280, 20131940. <https://doi.org/10.1098/rspb.2013.1940>

1585 Sues, H.-D., Fraser, N.C., 2010. *Triassic life on land*. Columbia University Press.

1586 Sun, Y.D., Joachimski, M.M., Wignall, P.B., Yan, C.B., Chen, Y.L., Jiang, H.S., Wang,
1587 L.D., Lai, X.L., 2012. Lethally hot temperatures during the Early Triassic
1588 Greenhouse. *Science* 338, 366–370. <https://doi.org/10.1126/science.1224126>

- 1589 Thomson, T.J., Droser, M.L., 2015. Swimming reptiles make their mark in the Early
1590 Triassic: Delayed ecologic recovery increased the preservation potential of
1591 vertebrate swim tracks. *Geology* 43(3), 215–218. <https://doi.org/10.1130/G36332.1>
- 1592 Valdiserri, D., Avanzini, M., 2007. A tetrapod ichnoassociation from the Middle
1593 Triassic (Anisian, Pelsonian) of Northern Italy. *Ichnos* 14(1), 105–116.
1594 <https://doi.org/10.1080/10420940601010703>
- 1595 Valentini, M., Conti, M. A., Mariotti, N., 2007. Lacertoid footprints of the upper
1596 Permian Arenaria di Val Gardena Formation (Northern Italy). *Ichnos*, 14(3–4),
1597 193–218. <https://doi.org/10.1080/10420940601049974>
- 1598 Xing, L., Klein, H., 2019. *Chirotherium* and first Asian *Rhynchosauroides* tetrapod
1599 trackways from the Middle Triassic of Yunnan, China. *Hist. Biol.* 11 p.
1600 <https://doi.org/10.1080/08912963.2019.1661409>
- 1601 Xing, L., Klein, H., Lockley, M.G., Li, J., Zhang, J., Matsukawa, M., Xiao, J., 2013.
1602 *Chirotherium* trackways from the Middle Triassic of Guizhou, China. *Ichnos* 20,
1603 99–107. <https://doi.org/10.1080/10420940.2013.788505>
- 1604 Xing, L., Klein, H., Lockley, M.G., Wu, X.-c., Benton, M.J., Zeng, R., Romilio, A.,
1605 2020. Footprints of marine reptiles from the Middle Triassic (Anisian-Ladinian)
1606 Guanling Formation of Guizhou Province, southwestern China: The earliest
1607 evidence of synchronous style of swimming. *Palaeogeogr. Palaeoclimatol.*
1608 *Palaeoecol.* 558, 109943. <https://doi.org/10.1016/j.palaeo.2020.109943>

1609

1610 **Figure captions**

1611

1612 **Figure 1.** Palaeogeographic maps depicting the global occurrences of Middle Triassic
1613 tetrapod tracksites (see Table S1 for references of the tracksites). **A.** Map of Pangaea at
1614 240 Ma modified from Alroy (2013). **B–C.** Anisian and Ladinian maps of the Western
1615 Tethys, modified from Manzanares et al. (2020) (see also references therein).

1616 **Figure 2.** Geographical and geological setting. **A.** Map of the Iberian Peninsula
1617 (modified from Escudero-Mozo et al., 2015 and Mujal et al., 2018a). **B.** Geological map
1618 of the Gaià-Montseny domain (modified from Ortí et al., 2018) with the location of the
1619 known tetrapod tracksites and other reference sections from the middle Muschelkalk
1620 facies. **C.** Synthetic stratigraphic sections of the middle Muschelkalk from the localities
1621 depicted in **B** with position of track levels.

1622 **Figure 3.** The Peña Rubí locality. **A.** Stratigraphic interval including the bulk of the
1623 tetrapod footprints on: the dolostone interval of the Arbolí Gypsum (lower arrow), and
1624 the first sandstone stratum of the Guanta Sandstone (upper arrow). **B.** Finely laminated
1625 dolostone bearing footprints of the Arbolí Gypsum, note the cyclic change of thickness
1626 of the laminae. **C.** Lateral equivalent of the dolostone in **B**, displaying cross lamination
1627 and being coarser (sandier). **D.** Ripples in red sandstones oriented in opposite
1628 directions, just above the track-bearing dolostone. **E.** Water escape and load structures
1629 within the red sandstones and mudstones just below the dolostone layers. **F.** Wrinkle
1630 structures resulting from desiccation of microbial mats (IPS106602). **G, H.** Footprints
1631 of *Rhynchosauroides tirolicus* preserved in finely laminated dolostones (IPS106601a;
1632 **G**), and relatively deeply impressed (IPS106617a; **H**).

1633 **Figure 4.** The Puigventós (**A**) and Montmany (**B–J**) localities. **A.** Common aspect of
1634 the Puigventós strata, being partially covered and fragmented. **B.** Sandstones, with cross
1635 stratification and ripples on top of each stratum, interbedded in red mudstones. **C.**
1636 Lateral section of IPS120437 displaying parallel lamination at the lower part and
1637 climbing ripples at the upper part; the arrow points to the section of *Sphingopus ferox*
1638 digit imprints. **D.** Left pes track of *Sphingopus ferox* (IPS120433) with the common
1639 preservation state of tracks in Montmany. **E.** Densely bioturbated sandstone including
1640 vertical and horizontal cylindrical burrows. **F.** Potential wrinkle structures of a
1641 microbial mat on a fine- to very fine-grained sandstone. **G.** Desiccation cracks. **H.**
1642 Potential gypsum moulds (partially recrystallised with calcite). **I.** Mould of a hopper
1643 crystal. **J.** Distinct massive carbonate layer (arrow), probably a dolostone, bearing
1644 abundant *Rhynchosauroides tirolicus* footprints, and likely corresponding to a portion of
1645 the Arbolí Gypsum embedded within Guanta Sandstone siliciclastic red beds.

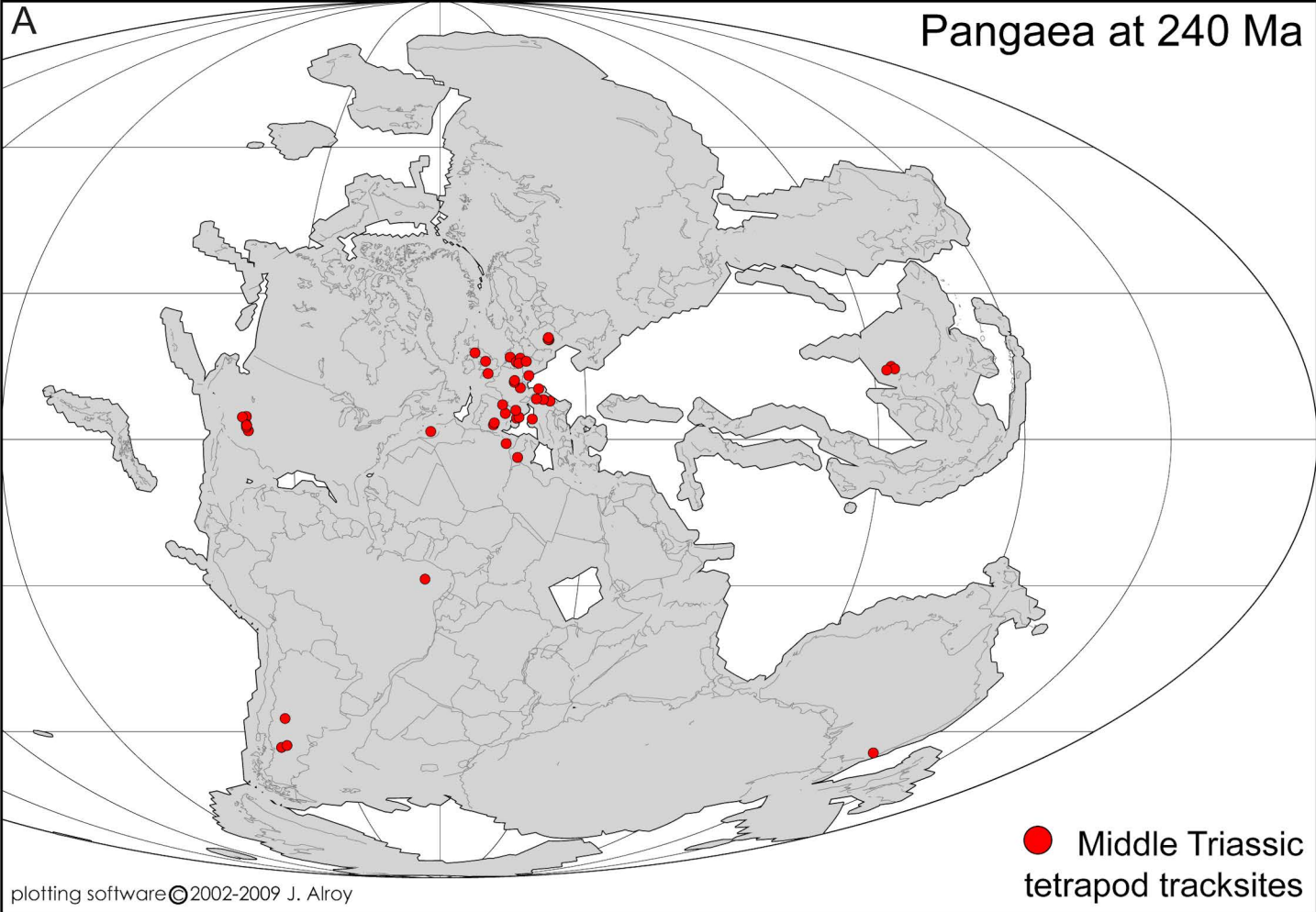
1646 **Figure 5.** Middle Muschelkalk (Catalan Basin) tetrapod tracks I. **A.** Left track of
1647 *Procolophonichnium haarmuehlensis* with skin impressions in convex hyporelief
1648 (IPS106601b). **B.** Small right track of *P.* isp. in convex hyporelief (IPS120440). **C.**
1649 Trackway of *Chelonipus* isp. in convex hyporelief (IPS110268). **D.** Right manus track
1650 of *Rhynchosauroides tirolicus* with skin impressions in concave epirelief (IPS106605c).
1651 **E.** Right manus-pes set of *Rh. tirolicus* in convex hyporelief (IPS106617b). **F.** Tiny left
1652 manus-pes set of *Rh.* isp. in concave epirelief (IPS120439). **G.** Left track of
1653 *Rotodactylus* isp. in concave epirelief (IPS107033b).

1654 **Figure 6.** Middle Muschelkalk (Catalan Basin) tetrapod tracks II. **A.** Two left manus-
1655 pes sets of *Chirotherium* cf. *sickleri* (with corresponding 3D colour-depth model) in

1656 convex hyporelief (MGSB-26310). **B.** Left pes track of *C. barthii* with skin impressions
1657 in convex hyporelief (IPS85803), arrows point to hopper crystal moulds. **C.** Left pes
1658 track of *Isochirotherium* cf. *coureli*, with *Rotodactylus* isp. tracks (arrows) and
1659 *Rhynchosauroides tirolicus* above digit IV, in convex hyporelief (portion of
1660 IPS110269). **D.** Right manus-pes set of *Sphingopus ferox* (with corresponding 3D
1661 colour-depth model) in convex hyporelief (IPS120435). Roman numbers refer to digit
1662 imprints.

1663 **Figure 7.** Occurrence of Middle Triassic tetrapod ichnotaxa and morphotypes based on
1664 Tables S1, S2 and S3. **A.** Percentage of occurrences of each ichnotaxon/morphotype
1665 within every defined palaeoenvironment; the number of total occurrences counted for
1666 each ichnotaxon/morphotype is above each bar; ichnotaxa and morphotype highlight in
1667 grey are those shown in **B**, whereas the rest are represented in “Others”. **B.**
1668 Ichnotaxon/morphotype relative proportions (percentages) in each palaeoenvironment;
1669 the graph shows the percentage that each ichnotaxon/morphotype represents in each
1670 setting; above each bar, the number of occurrences recorded in each setting is indicated.
1671 All ichnotaxa/morphotypes with less than 10 occurrences considering all
1672 regions/localities analysed (each being <4% of the total ichnodiversity) are included in
1673 “Others”. Data from both graphs correspond to presence/absence records of each
1674 ichnotaxon/morphotype without considering the absolute number of footprints from the
1675 analysed regions/localities.

1676 **Figure 8.** Idealised reconstruction of the Middle Triassic palaeoenvironmental settings
1677 showing the relative abundance of representative tetrapod (ichno-) taxa. Presence,
1678 distribution and relative abundance of tetrapod tracks is based on the references of
1679 Table S1, Fig. 7, and discussion in the text. Silhouettes are not to scale.



plotting software ©2002-2009 J. Alroy

